LAPPEENRANTA UNIVERSITY OF TECHNOLOGY
LUT School of Engineering Science
Master´s Degree Program in Chemical Engineering

*Avinash Bhandari*

# SYNTHESIS OF IRON-NANOPARTICLES FROM SOLID INDUSTRIAL WASTE FOR MINE WATER TREATMENT

Examiner: Professor Mika Sillanpää

Supervisor: MSc. Evgenia Iakovleva

## ABSTRACT

Lappeenranta University of Technology
LUT School of Engineering Science
Master's Degree in Chemical and Process Engineering

Avinash Bhandari

**Synthesis of iron-nano particles from solid industrial waste for mine water treatment.**

Master´s Thesis

2017

71 pages, 40 figures and 12 tables

Examiner: Prof. Mika Sillanpää

Supervisor: MSc. Evgenia Iakovleva

Keywords: Low cost adsorbent, acid mine drainage, adsorption, metal ions removal, uranium removal, arsenic removal.

Iron-nano particles were developed from solid industrial waste containing iron compounds and tested as potential sorbent for acid mine drainage (AMD) treatment. A simple cost effective treatment method to obtain iron nanoparticles was conducted using alkaline solution. Analytical instruments such as X-ray diffraction (XRD), Transmission electronic microscope (TEM), Fourier Transform Infrared spectroscopy (FTIR) and Brunauer-Emmett-Teller surface area analysis (BET) were used to characterize thus synthesized iron nanoparticles. This newly synthesized material proved high adsorption capacity towards common metal ions present in AMD such as Fe, Cu, Zn, Mn and As during removal study (pH dependence, kinetics and equilibrium experiments). Adsorption of these metal ions followed pseudo-second order model, which implies chemisorption. Batch adsorption experiments were performed in this work with synthetic mine water to find the optimum adsorption parameters. In addition to that, a column adsorption test was executed with continuous flow of synthetic and natural water for uranium and other pollutants removal. Inductively coupled plasma atomic emission spectroscopy (ICP OES) was used extensively for the determination of concentration of metal ions in the solution before and after adsorption. The result suggests a high potential for the studied material to be used as a low cost adsorbent for treatment of acid mine drainage.

**ACKNOWLEDGEMENTS**

Despite being the individual work, it could not have been possible without the help and support of number of people.

At this moment of accomplishment, first I would like to express my sincere gratitude to my examiner and laboratory head Dr. Mika Sillanpää for involving me in his project as a junior research assistant. I take this opportunity to acknowledge the financial, academic and technical support of Laboratory of Green Chemistry, Lappeenranta University of Technology.

I am also grateful to my supervisor MSc Evgenia Iakovleva for her continuous support, stimulating suggestions and encouragement during the thesis work. Thanks to her constant guidance and supervision for the completion of this work. One simply could not wish for a better and friendlier supervisor.

I would like to thank junior researcher Deepika Ramasamy for great discussions and immense help during the project work and also to all researchers from the lab for all fun we have made in last 6 months.

I would like to dedicate this work to my parents Ganga Ram Bhandari and Sita Devi Bhandari for their lifelong love, support and care. To my beloved wife Pratibha Koirala for constant love, understanding and encouragement. Also, to my brother and sister, who backed me to move on.

Finally, to all my teachers and classmates.

## TABLE OF CONTENTS

1. Introduction.....1
1.1. Objectives of the work ..... 1
2. Literature Review .....3
2.1 Mining Issues..... 3
2.2 Water in Mining ..... 4
2.3 Acid Mine drainage (AMD)..... 6
2.3.1 Acid mine drainage chemistry..... 7
2.3.2 Environmental impact of AMD..... 8
2.3.3 Prevention and trends in Acid Mine Drainage ..... 9
2.4 Treatment of Acid Mine Drainage..... 10
3. Adsorption.....17
3.1. Adsorption process ..... 17
3.3 Adsorption Isotherm ..... 21
3.4 Adsorbents ..... 22
3.4.1 Commercial adsorbents ..... 22
3.4.2 Low cost adsorbent ..... 24
3.5. Synthesis of iron-nano particles..... 26
4. Materials and Methods:.....27
4.1 Raw material and solutions..... 27
4.2 Chemicals ..... 27
4.3 Synthesis of iron nanoparticles ..... 28
4.4 Characterization of raw material and adsorbent..... 28
4.5 Adsorption experiments..... 30
5. Results and Discussions.....33
5.1 Synthesis of adsorbent..... 33
5.2 Characterization ..... 34
5.1. Batch experimental results ..... 37
5.2 kinetic study ..... 40
5.3. Isotherm study ..... 46
5.4. Column experimental results ..... 55
6. Conclusion .....59
References

## ABBREVIATIONS

| | |
|---|---|
| AMD | Acid mine drainage |
| $E_H$ | Electrochemical potential |
| XRD | X-ray diffraction |
| RH | Industrial sand (waste) |
| RH2M | RH material treated by 2M NaOH (Adsorbent synthesized in this work) |
| RH4M | RH material treated by 4M NaOH |
| BET | Brunaer-Emmet-Teller |
| FTIR | Fourier Transform Infrared Spectroscopy |
| TEM | Transmission Electron Microscopy |
| ICP OES | Inductively coupled plasma atomic emission spectroscopy |
| FBRs | Fluidized Bed Reactors |
| TOF-MS | Time of flight mass spectrometer |
| As(III) | Arsenic(III) |
| Cu | Copper |
| Fe | Iron |
| Zn | Zinc |
| Mn | Manganese |

# 1. Introduction

## 1.1. Objectives of the work

The main objective of this thesis work was to synthesize a low cost adsorbent from industrial waste for treatment of acid mine drainage. Acid mine drainage is a serious problem for aquatic and terrestrial lives and for the environment. Efficient and cost effective treatment of acid mine drainage is very important for mining industry. Keeping economic reasons into mind, non-conventional adsorbent has been studied instead of commercial adsorbent to minimize costs and cover small-scale processes.

Metallurgical solid wastes or industrial by-products are produced worldwide on large scales. Global industrial waste generation is around 10000 million tonnes per year (Tekes, 2012). These wastes has been proven economical and one of the most effective adsorbents in removing various pollutants. In this work, an industrial waste with commercial name (RH) provided by Ekokem Finland Oy is used as the base material for producing iron nanoparticles in order to treat acid mine drainage. This material contains higher amount of chemical components, including iron, aluminum, copper, zinc, cadmium and steel. Appropriate alkaline treatment of iron material present in this waste can induce iron nanoparticles. These nanoparticles or nano-adsorbents are highly valued adsorbents because they offer comparatively high specific surface area for adsorbates. Therefore, this work provides detailed study on synthesis, characterization of these iron nanoparticles along with adsorption studies on synthetic AMD.

The choice of metals used in this study was motivated by the fact that many constituents of acid mine drainage exists as cations, including most of the metals such as Cu, Zn, Mn, Fe, As (III), As(IV), Ni and Cd (Sheoran & Sheoran, 2006). Under strong acidic conditions these metals are highly mobilized in AMD ( (Saria et al., 2006). Beside these metals, arsenic is considered as the major pollutant and induces high contamination of AMD (Kagambega et al., 2014).

The synthesized adsorbent was further tested in column experiment for uranium adsorption. The permitted limit for uranium in water is from 15 to 30 $\mu gL^{-1}$, but in some region, it can be over that limit. For example, in some areas of California, USA, the water contains 2.5 $mgL^{-1}$ of uranium while in certain areas of southern Finland, the uranium content in water is around 7.8 $mgL^{-1}$, which is too high off the limit. In Finland, two largest deposits of uranium are found

in southern and northern region of Finland. Uranium is released into the environment during mining, processing, fuel manufacturing and spent fuel reprocessing (Maier et al., 2015).

# 2. Literature Review

Whenever, the surface and ground water is exposed to mine sites, it will dissolve primary and secondary minerals (Akcil & Koldas, 2006). This process is controlled by $E_H$-$p^H$ condition during mineral-water contact. Acid mine drainage have been a major source of environmental pollutant in mining regions around the world. The oxidation and dissolution of pyrites by water in presence of excess oxygen produce acidic and high metal ions content water. This highly toxic and acidic water is known as AMD, which is a threat to environment and most living organisms (EPA, 2016).

In AMD, the hazardous contaminants mostly contain reactive sulfides and are found in waste dumps, impoundments, leach pads, open cuts, pit walls and other exposed areas. These contaminants can be found in almost all mine sites including both underground and open pit mines (Kirby, 2014). New sources for AMD are continuously discovered due to time dependent behavior of AMD (Wolkersdorfer, 2008).

## 2.1 Mining Issues

Mining is the extraction of minerals or other important geological materials. There is a saying "Everything we use is either grown or mined" (Wolkersdorfer, 2008). Mining has been practiced since pre-historic times, but modern mining industry uses advanced tools for extraction, analyzes the profit potential of that desired mine and possesses minimum damage to environment (Wolkersdorfer, 2008). However, until today leakage or discharge of contaminated water from running or abandoned mine is seen as a global threat to water quality.

There is a fast growth in global mining industries due to the increase in demand for energy and mineral resources. As of 2014, total mineral production worldwide was 17 billion metric tons with a value of 5407.448 billion USD (Reichl et al., 2016). Only in Finland, 2 million metric tons of minerals were produced worth 5.339 billion USD (Reichl et al., 2016). The main products have been Cu, Ni, Zn, Co, Cr, Fe and V, while limestone, apatite, talc, quartz, feldspar and wollastonite are heavily mined for industrial mineral operations.

During mining, lowering of groundwater level is required to extract subsurface mineral resources and the removal of unwanted rocks to the surface as mine waste. Water in mining is used for extraction and processing of naturally occurring minerals on site. Water in contact with the mining or processing activities have their quality altered and produces potential

environmental and social impact. Huge amount of water is used in mining so higher probability of water resource pollution by discharged mine effluent and seepage from tailings exist (Kauppila, 2011).

## 2.2 Water in Mining

In mining sites, water is also continuously recycled and excess water is discharged from the site. Water in mining is mostly used for grinding and separation, but the usage varies with the mine types. Most of the water used is from self-extracted source, such as from mine dewatering, which occurs in the process of mineral extraction, rainfall, runoff and water infiltration. As mines need a stable and reliable supply of water, seasonal climate variability complicates the demand for mining water. During the dry season, limited local runoff and supplies of water from local resources will be restricted (Kauppila, 2011).

Environmental agencies in countries as if Finland, USA, Canada, etc. have limitations on water discharge for mine drainage based on taste, toxicity and concentrations of several element and compounds. Contaminated mine water can affect large areas for many decades. Treatment of contaminated mine water is often expensive in cases where faster treatment is needed at heavily populated areas and working mines (Kauppila, 2011).

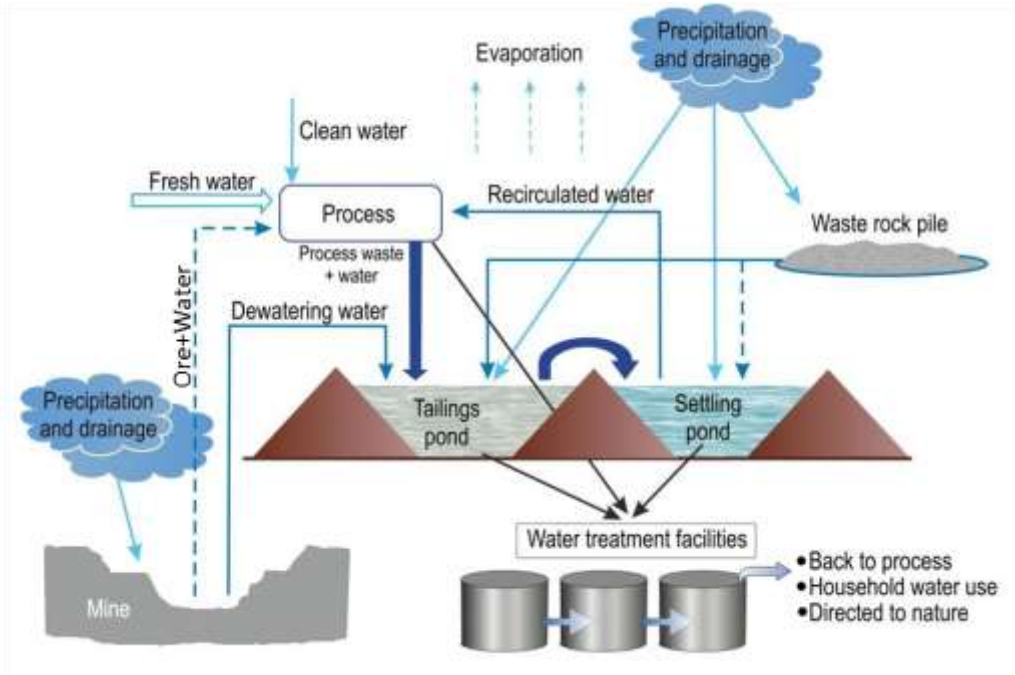


**Figure 1. Water cycle during mining operation. (Modified from** (Kauppila et al., 2011))

Water used in mining can be categorized into 3 types, such as process, natural and treated water.

*2.2.1. Process water.*

This includes water flowing in the plant and to be discharged effluent from the process. Water cycles and monitoring at the process plant is vital for the economy of the mining company and the plant water requirements are always during the mine-planning phase. In addition, the amount of discharged wastewater is set by plant process operations. These actions are important for the plant and the surrounding mine and its water systems (Kauppila et al., 2011).

*2.2.2. Natural waters.*

This category is for clean waters that include groundwater, surface water, rainfall, snowfall and water evaporation. These waters are fresh supply and may be diverted from the plant if not contaminated. Groundwater that is extracted during mine dewatering contains high concentrations of metals and metalloids as well as their possible salinity and the number of N-compounds, always require treatment. Therefore, the quality and state of these natural waters during their discharge to the natural water resources is the main focus ( Kauppila et al., 2011).

*2.2.3. Treated* water.

Treated water include the wastewater and treated waters during the mining operations. Tailings, ponds, as well as seepage waters consisting wastewater or used waters that may or may not require treatment. Figure 1 shows the treatment facility. Mining operations discharge waters with different qualities and in some cases, accidental spillages or leakage might occur, creating problems to the local aquatic environment. Accidents like rupture in the pipelines, overflow or seepage through the tailings pond barrier are likely to occur, which in turn can damage the structural integrity of the tailings dam (Kauppila et al., 2011).

There are mainly three types of mine wastewater based on their acid-base properties: acid mine drainage (AMD) with pH lower than 6, neutral mine drainage with pH at 6 or above and saline mine drainage with pH 6 and above that contains carbonates with concentration of more than 1000 $mgL^{-1}$ (Wolkersdorfer, 2008).

## 2.3 Acid Mine drainage (AMD)

AMD is formed when water flows over or through elevated sulphur contained materials forming stream with elevated proton acidity, higher metal concentrations (mainly Fe, Mn, Al, Ni) (Haunch, 2013; Sweeney, 2005). Moreover, seasonal variation and change in concentrations of metals also effects the acidity of wastewater (lower the acidity, higher the concentration). In addition to this, AMD generation is also favored by bacterial activities (Akcil & Koldas, 2006). AMD is a major source of pollution to surface water. The term AMD might be confusing to many with little knowledge on mine water chemistry, so the term used in literature means the contaminated discharge from mine sites especially coal mines (Haunch, 2013).

AMD is formed from sulphide metals, including pyrite and pyrrhotite that are present in the minerals. Once in contact with the air or water, these metals are oxidized eventually leading to sulfuric acid production and the liberation of metals (Kirby, 2014). Thus, the induced running water from these activities become acidic, carries along metals, and become acid mine drainage.

### 2.3.1 Acid mine drainage chemistry

In first reaction, ferrous, hydrogen and sulphate ions are formed by the oxidation of solid pyrite in presence of excess water and oxygen as shown in eq.1:

$$FeS_2 + \frac{7}{2}O_2 + H_2O \rightarrow Fe^{2+} + 2SO_4^{2-} + 2H^+ \quad (1)$$

Second reaction results in further oxidation of ferrous ion to ferric ion. This reaction acts as rate determining step, and reaction rate increases with increase in bacterial activities, due to pH dependence (Singer & Strumm, 1970).

$$Fe^{2+} + \frac{1}{4}O_2 + H^+ \rightarrow Fe^{3+} + \frac{1}{2}H_2O \quad (2)$$

The oxidized ferric ion reacts with water to give solid iron hydroxide and further increases acidity. Increase in pH above 3.5 results in precipitation of iron hydroxide leaving little unreacted ferric ions in the solution, simultaneously reducing the pH (Singer & Strumm, 1970)

$$Fe^{3+} + 3H_2O \rightarrow Fe(OH)_3 + 3H^+ \quad (3)$$

The remaining ferric ions acts as an oxidizing agent and oxidizes additional pyrite as shown in eq.4. This repeating reaction cycle continues until all ferric ions are consumed completely.

$$FeS_2 + 14Fe^{3+} + 8H_2O \rightarrow 15Fe^{2+} + 2SO_4^{2-} + 16H^+ \quad (4)$$

Considering this reactions, protons are generated thus releasing acid to the mine water. According to (Singer & Strumm, 1970), pyrite weathering is the major acid-producing mechanism in natural environment. Absence of buffering minerals, the acidity of AMD can go as low as pH 2.0 (Nordstrom et al., 1995). These reactions are exothermic in nature, thus the temperature of AMD can reach up to 40 $^{o}$C i.e. well above the normal temperature of natural water resources.

Bacterial activity is behind reaction 1 and 2 working as a microbial catalyst, while reaction 3 happens only after water leaves the mine. With the generation of proton from these reactions, pH decreases to around 4 and consequently pyrite oxidation is favored shown in reaction 4 (Wolkersdorfer, 2008). Various factors can influence the production of AMD such as the character of microorganisms, type of sulphide and non-sulphide mineral, ore or rock particle size, pH and conditions like availability of nutrients, water and oxygen (Evangelou, 1998).

### 2.3.2 Environmental impact of AMD

AMD is seen as a major cause of environmental pollution associated with mining industries. Beside its presence in active mine site, this can form even after years of mine closure (Kirby, 2014). It introduces acids and heavy metals into the environment well above the natural limit. Although, environment can adsorb the effects of AMD through dilution, biological action and neutralization but high-level pollution is too far from natural ability. These heavy metals can cause adverse effect on human beings and other living organisms and plants (Akcil & Koldas, 2006).

AMD has low pH, which is not suitable for aquatic life. Once spilled into the local water resource, its effect will be extend to distances. Water resource is the most affected natural resource by AMD, which allows the heavy metals to be consumed by aquatic life and by human through agriculture (EPA, 2016). Exposure to AMD can cause fish deaths as shown in figure below. The reason behind the fish death is due to loss of sodium ions in blood, which is induced by the increase permeability of fish gills to water, bringing less oxygen to the blood (Kimmel, 1983). Moreover, metals such as Cu, Zn, Mn and As which may be present in AMD are toxic even at low concentrations (Sangita & Prasad, 2010).


**Figure 2. AMD spills to Cuncumen River in Chile from Los Pelambres mine caused huge number of fish deaths. (Modified from** *(Patagonia, 2007)***)**

### 2.3.3 Prevention and trends in Acid Mine Drainage

A clear vision in tackling AMD crisis is required from both government and mining industry. Every day products for example from gadgets to home appliances all require valuable minerals from mining. However, to sacrifice environment and natural resources for these technologies is not a smart move. Mining industry must practice sustainability.

The objective of preventive techniques is to prevent the production of AMD. Despite many treatment methods currently used for AMD such as increasing pH, precipitation of metals and desalination to remove sulfate, the end quality is not consistent and generate a lot of waste. Mines with high concentration of pollutants in their area can see a huge increase in their cost for treatment of AMD, as long as AMD formation is prevented (Pozo-Antonio et al., 2014). Alternatives to treatment method can be the preventive methods such as (Motsi, 2010):

- Flooding/Sealing: Used mainly for abandoned mines by limiting supply of atmospheric oxygen.
- Underwater storage of mine tailings can be built in order to store and dispose potentially acid producing tailings.
- Sealing the open contaminated mine water by dry covers made from clay to prevent the movement of water.
- Blending acid consuming and acid producing materials producing environmentally viable product.
- Inhibiting the activity of AMD forming bacteria by using anionic surfactants called biocides.
- Covering mine with less permeable material such as fine-grained soil material, by products (fly ash, fluidized bed wastes), plastics. This can prevent rainwater from reaching this acid forming pyrites.

Probable solutions to minimize AMD in future could be to increase concern over water resource quality from both national and mining industry. Promoting sustainable use of mining minerals by recycle, reuse and looking for substitutes. Other important alternative would be to utilize industrial wastes for treatment of contaminated water (Ghali, 2014).

## 2.4 Treatment of Acid Mine Drainage

Despite AMD minimization and control remain as the main focus for mine water management strategies, but when mine water generation is unavoidable, efficient treatment technologies need to be implemented. Treatment technologies can be categorized as passive and active treatment methods, which combines physical, biological and chemical approaches (Taylor et al., 2005).

### 2.4.1 Passive Treatment Technology

Passive treatment method for AMD is purely focused on renovating and improving the quality of water that flow through the passive system (Zipper et al., 2011). Passive treatment deals with off-site treatment of mine water; it can be within the premise of mine area or can be at a certain distance from mine area depending on the treatment required, space and contaminants. An important factor that effects the design of passive treatment system is the quality of water to be treated (Weider & Lang, 1982). Water quality vary seasonally in most cases, so to have an effective passive system, the constituents of AMD from mine need to be measured for a certain period of time (Zipper et al., 2011). This information and knowledge of the discharge limit set by local government of authority determines the contaminants concentration and flow volume required. Passive treatment can be done by various methods, such as natural or technogenic beds, creating unfavorable environment for bacteria in waters, addition of lime and utilization of natural source.

#### 2.4.1.1 Anoxic Limestone Drains (ALD)

In this method, limestone is buried in oxygen-depleted trenches and mine water is transported into these trenches. This method works as limestone generate alkalinity and metal precipitation occurs followed by units like aeration cascade, pond or aerobic wetland so that precipitated metals can oxidize and easily removed. These trenches are covered by plastic liners, which in turn is covered by clay or compacted soil. This provides anoxic condition in the trench because presence of oxygen favors oxidation of ferrous iron to ferric and to ferric hydroxide. This technique controls acidity in mine water. (Skousen, 1991) (Innovation, 2014)

#### 2.4.1.2 Successive alkalinity producing system (SAPS)

This system is an extended form of anoxic limestone drains, which also involves porous organic material that produces anaerobic environment before water reaches the limestone. Organic substrate is kept on top of the limestone and mine water flows over it. Therefore, this system is kind of pond with 3 different layers (Skousen, 2000). Mine water flows through the organic substrate, where it is dissolved in organic matter to become more reducing and flows to the limestone where it becomes more alkaline and thus metals (aluminum, copper and iron) precipitation occurs. SAPS can treat acidity and reduce the concentration of these metals. (Innovation, 2014)

The role of organic matter is to create reducing conditions by stimulating the growth of sulfate and iron reducing bacteria.

#### 2.4.1.3 Aluminator

This is a modified SAPS technique, which is mostly for improving aluminum treatment but can also treat acidity and remove iron. In SAPS, an impervious cap is present in limestone drains to separate metals with water but Aluminator uses an organic layer and water instead (Innovation, 2014). This innovated system can work on high iron and oxygen concentration environment, increases pH, generate alkalinity and recovers aluminum. Specially designed perforated pipes collect the treated water and discharge. In addition to that, Aluminator has features to flush the system in order to get rid of precipitated aluminum buildup (Kepler & McCleary, 1994).

#### 2.4.1.4 Constructed Wetlands

These types of passive treatment systems use soil, wetland plants and crushed rock/media to build wetlands on the land surface. Constructed wetlands can operate as anaerobic-horizontal flow, aerobic and vertical-flow wetlands. This method can be useful in treatment of sulfate, different metals like Fe, Mn, As, Al, Cu, Zn, Cd, Se, Ni and Pb. In addition to that, it can treat acidic, neutral or alkaline mine drainage. (Innovation, 2014)

Wetlands can be designed as either subsurface flow or free water surface (Golder, 2009). In subsurface flow, the mine water flows through the granular media with aquatic plants on

surface of the media. In free water system, water flows over the surface of a planted treatment cell similar to natural wetlands. For the treatment of acid mine drainage, the wetland design must take into consideration factors such as disintegration processes, loading rate and hydraulic retention time, slope, substrate, vegetation, sediment control, geometric configuration, seasonal variation and local legislation (Rani et al., 2011).

#### 2.4.1.5 Biochemical Reactor (BCR)

This treatment method utilizes microorganisms to treat the contaminated mine water. Biochemical reactors can be constructed as open or buried ponds, in tanks, or in trenches between mine waste and a surface water body (ITRC, 2010). It can operate in high flows, highly acidic and metals loading, and passively or actively. BCR can treat metals such as Zn, Cd, Co, Ni and sulfates (EPA, 2014).

As this is a microbial treatment method, active BCRs require external liquid source of organic substrate and separate tanks or ponds for biological, chemical and physical processes. Passive BCRs employ solid reacting mixture as a carbon source for the bacteria and as a support for microbes and precipitation of metal sulfides. In passive BCRs, flow of mine water can be downward or upward or even horizontal, designed based on system transport and efficiency for removal of metals (ITRC, 2010). Naturally and locally available organic materials are used as organic substrate while availability and costs dictate the selection of organic carbon source such as liquid ethanol, manure, wood chips, fish bones, chitin, etc. (ITRC, 2008).

#### 2.4.1.6 Phytotechnologies

Phytotechnology or phytoremediation technology treat contaminated media with the help of plants and trees. Effective treatment include extraction of contaminants from soil or groundwater, control of hydraulics, runoff control, erosion and infiltration by vegetative covers. Contaminants that can be treated by this method are metals including Cr, and radionuclides including Ur, Ce and Sr (EPA, 2014).

In phytoremediation method, contaminants are concentrated in plant tissue; various biotic or abiotic processes degrade contaminants; volatile contaminants are released through leaf to air; plant roots are utilized to reduce the mobilization of contaminants in the root zone. For this

method to succeed appropriate plant species and soil amendment must be identified (USEPA, 2000). Phytoremediation helps in restoration and land reclamation during and after clean up (Innovation, 2014).

#### 2.4.1.7 Permeable Reactive Barriers (PRB)

In this method, contaminated water is treated by passing it through a reactive material on a permeable treatment zone. The reactive materials can be ZVI (ITRC, 2005), limestone, compost, zeolites, activated carbon and apatite and they are in direct contact with the surrounding aquifer. PRB has been successful in treating many different contaminants such as radionuclide, trace metals, and anions. Trace metals include hexavalent Cr, Ni, Pb, Ur, Tc, Fr, Mn, Se, Cu, Co, Cd and Zn whereas anion include sulfate, nitrate, phosphate and arsenic. (Innovation, 2014)

Two types of configuration of PRBs are in use: the funnel-and-gate and continuous PRB. Most commonly used is continuous, in which reactive material is backfilled in the trench. The trench is constructed perpendicular to and intersects a ground water plume. While funnel-and-gate design consists for impermeable walls such as sheet pilings, slurry walls as a funnel in order to make the contaminant plume flow to the gate containing reactive material.

### 2.4.2. Active Treatment Technology

Active treatment means continued operation, which involves regular human action along with either or both energy and chemical inputs. The aim of active treatment is to remove the pollutants in the mine water by physical processes (that involves filter or membranes) or chemical processes.

Most of the active treatment plant use chemicals to adjust the pH or $E_H$ value of the mine water in order to avoid the dissolution of metals. In acidic mine water, which is the most probable mine water case, reactants are added to neutralize or increase the pH of the contaminated water to a reasonable value that allows metals to precipitate.

Reactants such as caustic lime, sodium hydroxide and limestone are the most used chemicals for neutralization reaction (Skousen, 1991).

#### 2.4.2.1 Fluidized Bed Reactor

Fluidized Bed reactor also called pulsed or bed reactor can be aerobic or anaerobic that consists of granular solid media such as sand or granular activated carbon through which contaminated water passes at high flow rates enough to create mixed reactor configuration for biological growth or biofilm. Solids must be removed after biological treatment. Pollutants such as selenium, chromium, nitrate and perchlorate are treated by Fluidized bed reactor (FBRs) (EPA, 2014).

In this active treatment system, growth of microorganisms is fostered on a hydraulically fluidized bed of fine media, where velocity of passing fluid is tuned in order to suspend the solid media, which gradually increases the microorganism growth and contaminant treatment (Envirogen Technologies, 2011).

During FBR operation, reactor is first seeded with heterotrophic bacteria followed by pumping of electron donor materials and nutrients to foster the microbial growth. Next step is to pump the contaminated water into the FBR from the bottom so the fluid motion is upward direction to suspend the media. The growth of the microorganisms in the fluidized bed expands the bed height and after sometime a biofilm develops on the surface (CH2M Hill, 2010)

#### 2.4.2.2 Reverse Osmosis

It is a pressure driven separation process that involves semi-permeable membrane. When the contaminated water passes through the semi-permeable membrane, the dissolved ions are rejected while pure water passes through. The retentate is then disposed or treated. Despite reverse osmosis being a highly efficient method, construction requirement and operating costs limit its use.

Contaminants such as metals, total dissolved solids and sulfate are easily removed by reverse osmosis. In this method, pressure is applied on one side of the membrane high enough to overcome the osmotic pressure of water on the other side of the membrane, which then allows the separation. The contaminated water must be low in concentration of total suspended solids, calcium and magnesium. (Innovation, 2014)

#### 2.4.2.3 Rotating Cylinder Treatment (RCT)

This active treatment system is an advanced form of lime precipitation treatment. As described earlier lime is used to increase the pH and ease the precipitation of metals from the contaminated water (ITRC, 2010). In this system, contaminated water pass through shallow troughs that contain rotating perforated cylinders, which transfer oxygen and agitate the water, avoiding possible scaling of precipitated metal hydroxides and oxides. Rotating cylinder treatment system can precipitate metals, including aluminum, cadmium, copper, iron and zinc.

In RCT contaminated water is introduced to air in a thin film clinging to the rotating perforated cylinder (Ionic Water Technologies Inc.). As perforations impact water, it produces aggressive agitation and bubbles are forced into the water. This reduces the need for compressors and blowers. RCT unit is portable and can be sized to the requirements of individual sites. (Innovation, 2014)

#### 2.4.2.5 Electrocoagulation

Beside normal coagulation methods commonly used, this technique uses an electrical current to coagulate organic constituents and suspended solids present in mine water. In electrocoagulation, electrolysis is used with graphite or stainless steel as cathodes and metal as anode (Golder, 2009). Upon the application voltage, metals precipitate from the bulk and further filtration or sedimentation can remove precipitated metals from water. Constituents that are treated by this technique includes arsenic, copper, lead, zinc and cadmium along with phosphates and total suspended solids (EPA, 2014).

Electrocoagulation unit involves a chamber with a series of iron or aluminum plates, direct current is applied on either side of the positive and negative terminals, metals plates are electrified and metal ions are induced to wastewater flow, thus precipitate is formed. Electric current helps to destabilize suspended, emulsified or dissolved contaminants in the solution also provides electromotive force in driving the chemical reactions (CH2M, 2010).

#### 2.4.2.6 Ion Exchange

This is a reversible process of exchanging pollutant ions with desired ions from the solid surfaces of ion exchange resins (ITRC, 2010). Hardness and alkalinity removal, desalination, radioactive waste removal, ammonia and metals removal is possible by this technique.

In this method, water passes through ion exchange resins that takes four steps for completion of ion exchange process cycle: service, backwash, regeneration and rinse. Volume of service and backwash water can be higher so it may require for on-site storage tanks. Important parameters such as suitability and design of ion exchange system, resin type, volume and type of regenerant, backwash water source and quantities, requirement for pretreatment of solids, column configuration, pH adjustment and cycle length need to be optimized according to the requirement. (EPA, 2014)

#### 2.4.2.7 Adsorption

Adsorption is a process of concentrating polluted ions from bulk solution to the surfaces of a porous solid. The porous solid is called adsorbent while the concentrating ions or particles are called adsorbates. The movement of particles from bulk solution to the surface of adsorbent is mainly due to the surface charge present on the adsorbent surface so the choice of adsorbent should be made based on the charge of ions (EPA, 2014).

Among all active treatment methods, adsorption is a very cost effective and efficient treatment method with simple and stable operation, less effort for handling waste, no added reagents, compact facilities and usually low operation cost (Akin et al., 2012). Different types of commercial and low cost adsorbent are available. Largely available natural materials or waste products from industries can potentially be used as low cost adsorbent.

### 2.4.3 Comparison between passive and active treatment method.

Passive methods are less expensive compared to active treatment. However, due to certain drawbacks, it has limited use in the modern mining industries. Main drawbacks are inability of this method to remove metals such as zinc (Wolkersdorfer, 2008), and longer process time, which is not suitable for high influx of mine water during intense mine works (Iakovleva et al., 2013).

Passive treatment of acid mine drainage is time consuming and sometime does not match the output water regulation. Active treatment is however better and faster than the passive treatment but is costly. Construction and operational costs and chemical costs are higher for active method. Adsorption is one of the active treatment method, which is cost effective and possess great potential for the treatment of acid mine drainage. Further reducing the cost of adsorbent, energy and amount of adsorbate will surely make adsorption a cost effective active treatment method for acid mine drainage.

# 3. Adsorption

Sorption is defined as the surface phenomena where change in concentration of a substance or chemical substance occur at the common boundary of two phases, which can be due to absorption, adsorption and ion exchange. In absorption, substance is chemically bonded or is inside the substrate while in adsorption, the substance is physically bonded on the surface and in ion exchange, the movement of ions occurs on the boundary surface, usually liquid phases.

The term adsorption was first introduced in 1881 for prediction of condensation of gases on free surfaces (Gregg & Sing, 1982) . Adsorption is a physical and chemical separation process where particles or materials (adsorbate) are concentrated from bulk vapor or liquid phase on to the surface of a porous solid (adsorbent). “Positive” adsorption meaning interfacial concentration of the adsorbate is greater than in bulk phase or decrease in interfacial energy, while “negative” adsorption increase the interfacial energy of the system. Adsorption can be classified into physisorption and chemisorption depending upon the nature of bonds, between the adsorbent and adsorbate. Bonds such as Van der Waals, hydrogen bond, hydrophobic and weak electrostatic interactions are responsible for physisorption while covalent and ionic bonds are responsible for chemisorption. (Oleksiienko, 2016)

In physisorption, long range and weak Van der Waals attraction between adsorbate and adsorbent occur with change in enthalpy (ΔH) to be about 20 KJ/mol. It does not have activation barrier, is reversible and can be monolayer or multilayer at a temperature near to the critical temperature (Kleiman & Landman, 1973). In chemisorption, short range and strong bonding between adsorbate and adsorbent occur with change in enthalpy (Δh) about 200 KJ/mol. This is usually irreversible, only monolayer formation is possible, has specific surface symmetry and consists of activation barrier.

## 3.1. Adsorption process

Two aspects that can be considered in adsorption process: Thermodynamics, which relates to final equilibrium interfacial energy and Kinetics, which dictates the rate of adsorption process (NCKU, 2015). Mine water treatment is a complex process that require various stages and among all the treatment techniques, adsorption is one of the low cost treatment method that can be used for wide variety of pollutants (such as anions, metals, arsenic, mercury, radioactive elements, and many others) (Iakovleva & Sillanpää, 2013). Although, adsorption cannot

replace the current methods, it can be used an alternative to other methods. Adsorption has certain advantages over other techniques such as ability to separate selected compounds from dilute solutions, simple design, operational simplicity and easy scale up, high capacity and favorable rate, insensitive to toxicity (Soto et al., 2011). Adsorption also enables recovery of adsorbed compounds by desorption, leaching, biological treatment and thermal treatment (Kikuchi & Tanaka, 2012).

Various mathematical models have been developed to describe the adsorption kinetic, which can be divided into adsorption reactions models and adsorption diffusion models. Adsorption diffusion model deals with time-dependent adsorption on solid surfaces. There are four stages that can determine adsorption kinetics by diffusion model: external diffusion, internal diffusion, surface diffusion and adsorption/desorption process. Adsorption reaction models derived from chemical reaction kinetics are based on the whole adsorption process excluding the above four stages.

Factors affecting rate of Adsorption are:

- Effect of adsorbent mass

  Increase in adsorbent mass increases the adsorption of the heavy metals. This is due to availability of more adsorption sites for adsorbates.

- Effect of particle size

  In a particle or adsorbent, surface area plays an important role in adsorption. Uptake of metals from bulk solution usually occurs at sites on the outer surface of the particle as well as sites within the particle. Intraparticle diffusion resistance limits the accessibility of metals ions to the internal adsorption sites due to which only part of these sites is available. In order to increase the number of accessible sites for metal uptake, external surface area must be increased, while reducing the adsorbent particle size (Inglezakis et al., 1999). Reducing the particle size also create shorter diffusion distance for heavy metals, resulting faster reaction rate.

- Effect of initial solution pH

  The pH of the solution in contact with the adsorbent has an effect on the adsorption capacity towards the metal cations due to the influence of acidic solution on the character of metal ions and adsorbent. At lower pH, $H^+$ ions compete with cations for same free sites hence

decreasing the removal efficiency of heavy metals (Motsi, 2010). In addition to that, increased adsorption of $H^+$ ions produce positive charge on the surface of adsorbent resulting in repulsion of metal cations (Cabrera et al., 2005).

- Effect of initial solution concentration

  During the adsorption process, increase in initial concentration of heavy metals increases their adsorption and the rate of adsorption. The relative increment will continue until the system reaches to a point, after which further increase in concentration of heavy metals will not have any effect in the amount adsorbed (Motsi, 2010).

- Effect of agitation

  Agitation is vital parameter in adsorption that helps in reducing the external mass transfer resistance. During agitation or stirring, the thickness of liquid film layer surrounding the adsorbent reduces, which in turn increases the mass transfer of diffusing metal ions resulting in higher metal uptake. Agitation not only helps to overcome mass transfer resistance but also results in abrasion of adsorbent grains, producing new reactive locations on the surface. Therefore, agitation provides new adsorption sites on the surface, promoting the rate of adsorption. Despite these positive effects, abrasion of particles results in fine particles, which can be very difficult to separate from the liquid (Inglezakis et al., 1999).

- Effect of competing cations

  Acid mine drainage comprises of many different metal ions as a mixture. This variety will affect the efficiency of an adsorbent in treating AMD. The affect will be due to the competition for the adsorption sites on and in the adsorbent (Motsi, 2010). It is therefore important to analyze the influence of competing cations on the removal of each metal from the solution.

- Effect of thermal pre-treatment

  Thermal pre-treatment can result in increased adsorption due to removal of water from internal channels of an adsorbent. However, overheating may damage the porous structure reducing the adsorbing capacity (Akdeniz & Ulku, 2007). The adsorption capacity decreases as the metal cations will not have available sites within the adsorbent.

## 3.2 Kinetic Models

Kinetic study is important to understand the adsorption rate of adsorbates. Based on the literature review, two types of kinetic models are commonly used pseudo first order and pseudo second order equations. In order to determine the kinetics behind adsorption of each metal ions, pseudo-first order and pseudo-second order models can be applied. In this study both linear and non-linear forms of pseudo first and second order equations were used. The pseudo-first order model in non-linear form and linear form is given by equations 4 and 5 respectively,

$$\frac{dq}{dt} = k_1(q_e - q) \quad (4)$$

$$ln(q_e - q_t) = lnq_e - k_1 t \quad (5)$$

Where $k_1$is the pseudo-first order rate constant ($min^{-1}$) and $q_e$(mg/g) is the adsorption capacity at equilibrium and $q_t$(mg/g) is the amount of metal adsorbed any time t. The plot of $ln(q_e - q_t)$ vs *t* will give a straight line with slope $k_1$ and intercept $lnq_e$.

Pseudo second order model in non-linear and linear form is given by equations 6 and 7,

$$\frac{dq}{dt} = k_2(q_e - q)^2 \quad (6)$$

$$\frac{t}{q_t} = \frac{1}{k_2 q_e^2} + \frac{1}{q_e} t \quad (7)$$

Where $k_2$(g $mg^{-1}$ $min^{-1}$) is the pseudo-second order rate constant. Plot of *t/q* vs *t* gives slope of $\frac{1}{q_e}$ and intercept $\frac{1}{k_2 q_e^2}$.

For non-linear fitting in both models, using excel solver, $q_e$ and *k* values were estimated by minimizing the sum of the errors. Error is the square of difference between experimental $q_t$ and calculated $q_t$ as shown below:

$$\sum_{i=1}^{n}(q_{t,exp} - q_{t,cal})^2 \quad (8)$$

## 3.3 Adsorption Isotherm

Adsorption isotherm provides the information about the amount of adsorbate adsorbed on the adsorbents from a solution of defined concentration at equilibrium and constant temperature. In other words, isotherm shows the adsorption capacity of certain adsorbents. Originally, adsorption isotherms were utilized in gas and vapor adsorption where the adsorption equilibrium was expressed as a function of gas or vapor pressure. Later, replacing pressure with equilibrium concentration, isotherms were also applied for adsorption of solutes (Worch, 2012).

There are mainly 4 classes of isotherm models: S curves represents vertical orientation of adsorbate at the surface. L curves represents Langmuir isotherms with both flat and vertical orientation of adsorbates with strong intermolecular attraction. H curves represents mostly to the adsorption due to ion exchange and C curves are linear curves, which represents the solutes that penetrates solids more easily than solvents. The subgroups are arranged according to the shape, plateau and slope of the isotherm. Among these isotherms, L2 type (inside red box) is most common and occurs in majority of cases of adsorption from aqueous solution.

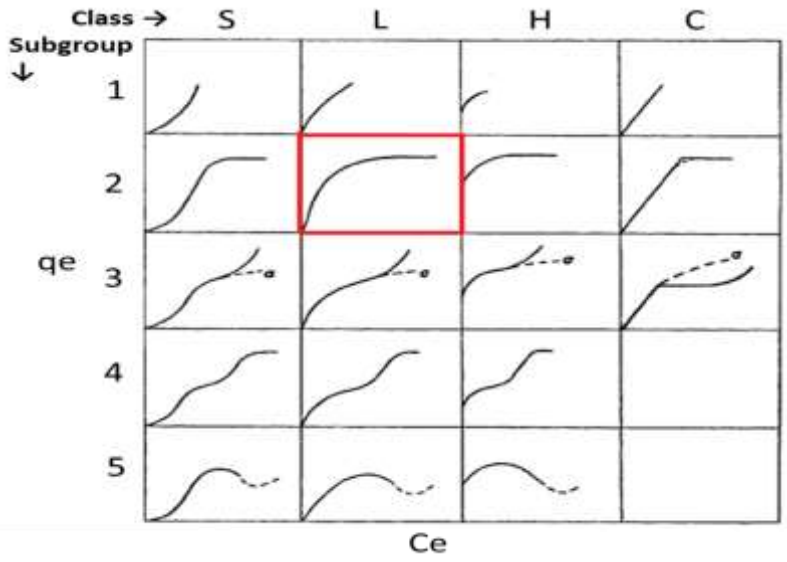


**Figure 3. System of isotherm classification. Modified from** *(Giles et al., 1960)*

Langmuir isotherm model is used for describing monolayer adsorption onto a homogeneous surface with definite adsorption sites (Giles et al., 1960). This model assumes that there is a uniform energy distribution for adsorption over the surface and no interaction between adsorbed molecules. This isotherm model is determined by following equation,

$$q = q_s \frac{bc}{1+bc} \quad (9)$$

Where $q$ is the maximum adsorption capacity, $q_s$ is saturation capacity, $b$ is Langmuir constant and $c$ is the concentration of adsorbate.

Freundlich isotherm model is described for multilayer adsorption onto a heterogeneous surface that assumes there is non-uniform energy distribution for adsorption over the surface (Giles et al., 1960). Freundlich isotherm can be determined according to equation,

$$q = q_s \frac{bc^n}{(1+bc^n)} \quad (10)$$

Where, Where $q$ is the maximum adsorption capacity, $q_s$ is saturation capacity, $c$ is the equilibrium concentration of adsorbate $b$ and $n$ are Freundlich constants.

## 3.4 Adsorbents

Selection of adsorbents based on the adsorbate-adsorbent characteristics is the most important task in order to achieve a good adsorption. Availability, low cost, non-toxicity, corrosiveness and minimum loss in performance with easy regeneration steps should be considered while making the selection.

Properties of adsorbent such as porosity and surface area determines its adsorption capacity. A good adsorbent has high porosity and larger surface area that provides more space for adsorbates. Most of the adsorbents are porous in nature, which increase the surface area and the kinetics of the adsorption so it requires less time for adsorption equilibrium (Bhatnagar & Minocha, 2006).

### 3.4.1 Commercial adsorbents

#### 3.4.1 Activated carbon

Activated carbon is the widely used commercial adsorbent. It has high surface area, microporous structure and higher adsorption capacity (Satyawali & Balakrishnan, 2008). The major carbon sources for activated carbon are nutshells, peat, wood, coir, lignite, coal and petroleum pitch (Iakovleva & Sillanpää, 2013).

Although, activated carbon has great potential in removing heavy metals through adsorption, high cost and 10-15% loss during regeneration has limited its use (Vimal et al., 2006). In addition to that, commercial activated carbon need complexing agents to increase its removal efficiency. Therefore, small-scale industries are no longer attracted to it due to cost inefficiency. The high price (about 500-1800 USD per metric ton) of activated carbon is limited its using,

#### 3.4.1.2 Activated alumina

Activated alumina is produced from aluminum hydroxide by dehydroxilation under carefully controlled conditions. This gives a highly porous structure having higher surface area significantly over 200 $m^2g^{-1}$. Applications of this compound are as a drying agent and as a sorbent for removal of fluoride, arsenic (Merta, 2015) and selenium (Reinsel, 2016) from drinking water.

It has been widely used in filtration of fluoride from drinking water in places with heavy concentration of fluoride in water for example in Jaipur region, India, where the concentration is enough to cause fluorosis (Iakovleva & Sillanpää, 2013).

#### 3.4.1.3 Zeolite

Zeolites are porous aluminosilicate minerals with high surface area and high affinity towards ions such as Pb, Cu, Cd, Zn, $UO_2$, etc. The number of $[AlO_4]^{5-}$ tetrahedral determines the number of cations in zeolite. Substitution of $Al^{3+}$ for $Si^{4+}$ in the structure results in the net negative charge, which must be counterbalanced by cations (Alvarez et al., 2003).

Natural zeolites can contain contaminants from minerals and may not be suitable for all applications so synthetic zeolites are produced (Panek et al., 2011). Prices range from $400-500 per metric ton. Various research has been done with different zeolites for purification of acid mine drainage (Rios et al., 2008; Gaikwad et al., 2011; Motsi, 2010; Motsi et al., 2009).

#### 3.4.1.4 Silica gel

Silica gel is prepared by dehydrating geothermal water containing silicic acid (Yokoyama et al., 2002). Silica gel adsorbs gas or vapor effectively from organic substances along with water. Therefore, it has found its usage in adsorption of gasoline, benzene, ether, acetone, etc. vapors from air and natural gas (Amini et al., 2011). With its polarity and high surface area around 100 to 750 $m^2g^{-1}$, it is comparatively higher than activated carbon. So, research has also been

done in using silica gel in aqueous system. Several works has been done in this area (Repo et al., 2011; Repo et al., 2011), but one major drawback is that silica gel is not biodegradable in either water or soil.

### 3.4.2 Low cost adsorbent

#### 3.4.2.1 Biosorbents

These adsorbents are comprised of naturally available agricultural residues, algae and microorganisms. Modified biosorbents have shown good metal binding capacity forming complexes or chelates due to the presence of acetamido, alcoholic, carbonyl, phenolic, amido, amino, and sulfhydryl functional groups. Microbial cells offer high affinity towards metal ions although metal uptake efficiency differs between non-microbial, microbial biomass and between the microbial species. Locally available industrial by-products and natural materials can be used as low-cost adsorbents. Some of them include shells, peat moss, seaweed/algae, dead biomass, etc. (Bailey et al., 1999).

#### 3.4.2.2 Municipal sewage sludge

Municipal sludge contains high concentration of carbon, which makes it an interesting material as adsorbents. It has a high surface area and can be considered as a low cost adsorbent. The potential application of this sludge has been studied in the field of metal ions and organic compounds adsorption. Activation is the major part for these adsorbents, which can include carbonization, physical and chemical activation or combination of both. Activation by pyrolysis (Filippis et al., 2013) and modification by iron oxide (Phuengprasop et al., 2011). A review carried out by (Bhatnagara & Sillanpää, 2010) for the application of sewage sludge shows interestingly higher adsorption capacities for treatment of pollutant in wastewater.

#### 3.4.2.3 Limestones

Acid mine drainage requires the addition of alkalinity to it; limestone is one of the least expensive alkaline source. Limestone is the most cost effective material for acid neutralization but drawbacks such as slow rate of dissolution under atmospheric condition and tendency to armor with ferric hydroxide made its use rare. Various researches has been done on limestone treatment of AMD (Silva, 2012; Iakovleva, et al., 2015; Watten, 2005; Strosnider & Nairn, 2010) in removing metal ions. (Iakovleva et al., 2015) modified limestone with NaCl and mine process water, and found a significantly good adsorption of dissolved metal ions from AMD.

#### 3.4.2.4 Iron containing waste

Industrial waste or waste from other mining sites can be used as a possible adsorbent for acid mine drainage. Industrial wastes have shown a good adsorption capacity towards heavy metals such as Zn, Cu, Cr, Mn, etc. Iron containing adsorbents have been studied by many researchers. (Nguyen et al, 2016) have used natural iron-rich sandy soil for removal of lead from water, (Hamza & Fashola, 2014) have used calcined iron rich clay for degradation of phenol in water, (Nguyen, 2009) have used iron mining waste for the removal of arsenic from water. Ferrihydrite and zero valent iron has been used for adsorption of metal ions from wastewater. Ferrihydrite adsorption is mostly used for removing heavy metals mostly selenium and arsenic and also metals that can co-precipitate. This technique involves first the addition of ferric salt into the mine water, which produces ferric hydroxide and ferrihydrite precipitate: this formation results in the adsorption of metals on the surface (CH2M Hill, 2010). The precipitated iron can be removed and requires other treatment for disposal. This method is widely used in mining industry (EPA, 2014).

In active mine water treatment, zero valent iron (ZVI) can be used in neutralizing acids and promoting removal and immobilization of dissolved heavy metals through adsorption. Contaminants such as selenium, arsenic and radionuclides are treated by ZVI. Selenium oxyanions can be reduced to elemental selenium, ferrous cations can reduce selenite to selenite and finally removed by adsorption to iron hydroxides (Innovation, 2014). In mine water treatment, ZVI act as a reducing agent and also as a catalyst and an electron donor. Anoxic condition is preferred for treatment and multiple tanks can be used in series to increase treatment (CH2M Hill, 2010).

Iron rich industrial waste such as iron sand can work over wide range of acidity, is low cost and requires inexpensive regeneration. The surface of these adsorbents can be activated by treating them with alkali solutions. Treatment with alkali solution provides more -OH and possible Fe-0 groups on the surface which increases the adsorption ability towards positive ions. Various researchers (Mukherjee, et al., 2015; Machado, et al., 2014; Natarajan & Ponnaiah, 2010) have reported the production of iron nanoparticles from industrial waste for treatment of different metal ions in wastewater. Iron nanoparticles are very interesting due to their magnetic properties, high surface area and tendency to bind cations. These nanoparticles can be prepared by several methods such as chemical precipitation, selective leaching and thermal decomposition.

## 3.5. Synthesis of iron-nano particles

### 3.5.1 Co-precipitation method

This is known as the classical synthesis method for producing $Fe_3O_4$ (magnetite) iron nanoparticles. In this method, a mixture of ferrous and ferric salts is aged in an aqueous solution. An alkaline aqueous medium is used to precipitate the ferrous and ferric ions at solution pH between 8 and 14. The stoichiometric ratio should be 2:1 ($Fe^{3+}$: $Fe^{2+}$) and should be produced in non-oxidizing environment. Magnetite is unstable and oxidizes to form maghemite ($\gamma Fe_2O_3$) (Laurent et al., 2008).

### 3.5.2 Thermal decomposition

High-quality superparamagnetic and monodispersed magnetite nanoparticles have been synthesized by this method (Sun & Zeng, 2002). The reaction is performed at high temperature (200 $^oC$) and pressure (2000 psi) in a reactor or autoclave. The nanoparticles are obtained through decomposition of iron precursors such as $Fe(Cup)_3$, $Fe(CO)_5$ or $Fe(acac)_3$ at higher temperature by using organic solvents and surfactants such as oleic acid, oleylamine or octyl ether (Laurent et al., 2008).

### 3.5.3 Sol-Gel method

This is a wet route process for synthesis of iron nanoparticles. The terms sol here represents the process of hydroxylation and condensation of precursors in the solution of nanoparticles. While gel represents the three-dimensional oxide network formed by the condensation and inorganic polymerization of sol. Thus, formed nanostructures are amorphous and further treating at 400 $^oC$ gives the crystalline structure (Laurent et al., 2008). $\gamma$-$Fe_2O_3$ nanoparticles has been synthesized by (Monte et al., 1997) through heat treatment of gels at 400 $^oC$.

# 4. Materials and Methods

## 4.1 Raw material and solutions

The raw material for synthesizing adsorbent in this study was received from Ekokem Finland. The commercial name for this material was RH and same name was continued in this work. It was provided in the form of powder with the presence of big and small particle sizes. The chemical composition of original RH material is shown in table 1. RH material contains about 10% (w/w) iron. Iron does not remain as a free element but oxidizes or combines with other compounds or molecules.

**Table 1. Chemical composition of RH with XRF analysis**

| Element | Wt % |
|---|---|
| Si | 0.2 |
| S | 17.6 |
| K | 0.3 |
| Ca | 14.4 |
| Fe | 10 |
| Compounds formula | $Ca(SO_4)(H_2O)$; $Na_2Al_2Si_3O_{10}$ |
| Compounds name | Calcite; Zeolite |

Two types of synthetic solution were used here in this work. Metal salts solution containing Fe, As, Cu, Mn and Zn ions were used as a synthetic AMD during the batch experiments. For the column experiment, solution containing Fe, U, Pb, Cr, Zn, Cu, Cd, Mo and Se ions was used. Natural lake water was also used for column experiment.

## 4.2 Chemicals

Synthetic AMD solutions of Fe (II), Cu (II), Zn (II), Mn (II) and As (III) were prepared from $FeSO_4.7H_2O$, $CuSO_4{\cdot}5H_2O$, $ZnSO_4{\cdot}7H_2O$ , $MnCl_2{\cdot}H_2O$ and $As_2O_3$ respectively (obtained from Sigma Aldrich). Alkaline solution prepared from sodium hydroxide (obtained from Merck) was mostly used for synthesizing iron nanoparticles. Synthetic mine water for column experiment was prepared from multielement standard solution (Sigma-Aldrich) containing various concentrations of Fe, U, Pb, Cr, Zn, Cu, Cd, Mo and Se elements.

## 4.3 Synthesis of iron nanoparticles

In order to synthesize iron nanoparticles, RH was sieved to 200-µm size, washed with distilled water and dried for 12 hours at 80 C. For sieving, laboratory test sieve (Endecotts Ltd. London) of 200-µm mess size with steel frame and steel mess was used, Milli-Q Ultrapure water was used for the washing. After RH material was dried, it was mixed with 1, 2 and 4M sodium hydroxide (1:6 ratio) solution and cooked for 2 hours under continuous mechanical stirring at 70 C. The treated adsorbent was then washed 4 times thoroughly with distilled water and dried in the oven at a temperature of 120 C for 5 hours. For this work, 2M NaOH solution was considered optimum based on the result from various characterization techniques described more below. Thus, new synthesized adsorbent containing iron nanoparticles is named as RH2M.

## 4.4 Characterization of raw material and adsorbent

### 4.4.1 BET

BET (Brunauer-Emmet-Teller) analysis explains the physical adsorption of gas molecules on adsorbent and allows multilayer adsorption. This provides us the specific surface area and pore characteristics for the materials analyzed. Adsorbents were first dried along with continuous purging of nitrogen gas. Once the sample were dry, the Nitrogen-adsorption-desorption isotherm of the modified adsorbents were measured by the Micromeritics Instrument.

### 4.4.2 XRD

X-ray diffraction (XRD) patterns of original and modified (containing iron nanoparticles) were collected over a 2θ range 15–100° and at fixed divergence slit 0.76 mm with the help of PANALYTICAL X-Ray diffractometer using Co Kα (= 1.78901 Å) radiation.

### 4.4.3 FTIR

The FTIR spectra of original and modified RH were measured in the range 4000–400 $cm^{-1}$ by using a Fourier transform infrared spectrometer (FTIR, VERTEX70, Bruker Optics, Germany). FTIR analysis was done for both activated or modified and original RH adsorbents

### 4.4.4 TEM

TEM images of α-FeOOH nanoparticles were collected by transmission electron microscope (TEM) with an accelerating voltage of 100 kV (Hitachi 7700).

### 4.4.5 ICP OES

Concentration of metal ions in the original and treated metal ions solutions were analyzed by Optical Emission Spectroscopy (ICP OES) spectrometer iCAP 6000 Series, Thermo (UK). It has detection limit for most of the metals at ppb scale.

### 4.4.6 TOF MS

Time of flight mass spectrometer (TOF MS) with pulsed glow discharge ionization in combination with hollow cathode source is a high sensitive analytical instrument for direct determination of trace amount element from solid sorbent. This is a low cost, fast and efficient technique to analyse element and isotope in solid samples. Elemental and isotope analysis of geological samples was carried out using TOF MS for the first time by (Iakovleva et al., 2016, under review) with pulsed glow discharge ionization in combination with hollow cathode course Lumas-30 (Lumass Ltd, St. Petersburg, Russia). In this work, this instrument was used for direct analysis of sorbents before and after natural and synthetic mine waters treatment.

## 4.5 Adsorption experiments

Adsorption studies were conducted through batch experiments. Several batch tests were performed with several metal ions (Fe, Cu, Zn, Mn and As) solution and synthesized adsorbent (RH2M) studying the effect of variables such as initial pH, contact time, adsorbent mass, temperature and initial solution concentration.


**Figure 4. Batch adsorption experiment carried out in plastic tubes with a mechanical shaker.**

### 4.5.1 Effect of initial pH

In adsorption processes, pH is well known key parameter due to its influence not only on metal speciation but also on the surface ionization state. For this experiment, a synthetic solution was prepared using $As_2O_3$, $MnCl_2{\cdot}H_2O$, $ZnSO_4{\cdot}7H_2O$, $FeSO_4{\cdot}7H_2O$, and $CuSO_4{\cdot}5H2O$. The initial concentration of all elements (As, Mn, Zn, Fe and Cu) was set to 25 ppm. Therefore, in order to achieve 25 ppm of each element in the solution (50 ml), required amount of metal salts were calculated and weighed using balance. They were then mixed with 50 ml of ultrapure water. To analyse the effect of initial solution pH (3, 4, 5, 6 and 7), 5 * 50 ml solution was prepared for each element with 25 ppm concentration. In order to adjust the pH, 0.1 M HCL and 0.1 M NaOH buffer solutions were used. So, there were 5 samples for each element at different pH totalling to 25 samples. Out of 50 ml, 10 ml each solution was taken and stored in plastic tubes for adsorption experiment.

10 mg of the RH adsorbent was put into the tubes containing 10 ml of each of those 25 samples and then were mixed using mechanical shaker for 18.5 hours at 100 rpm at room temperature. After that, they were filtered using 0.2 µm syringe filter. 5 ml of each sample was then used for ICP analysis.

Calibration solutions (1, 5, 10, 15, 25 & 50 ppm for each metal ions) for determination of metal ions by ICP were prepared from standard solutions with initial concentration of metal ions 10000 ppm. These were dissolved in 10% $HNO_3$.

### 4.5.2 Effect of adsorbent mass

To analyze the effect of adsorbent mass on the adsorption of different elements, various mass of adsorbents were taken. The mass were 0.5 $gL^{-1}$, 1 $gL^{-1}$, 2 $gL^{-1}$, 5 $gL^{-1}$, 10 $gL^{-1}$, 15 $gL^{-1}$, 20 $gL^{-1}$, 25 $gL^{-1}$, 30 $gL^{-1}$, 35 $gL^{-1}$ and 40 $gL^{-1}$.
For every metal, we had 11 different mass of adsorbents, totaling to 55 samples for 5 metals. The metal solution concentration was kept at 25 ppm for each metal and at constant pH of 6. For the adsorption test, 15 ml of each metal solution was taken and mixed with respective adsorbent mass from 0.5 $gL^{-1}$ to 40 $gL^{-1}$ in a plastic tube. All of the samples were then put on a shaker for 24 hours at 100 rpm in room temperature.

After that time, all the samples were filtered using syringe filter (0.2 µm) and 10 ml of that was stored in test tubes for ICP analysis.

### 4.5.3 Effect of contact time

For this experiment, 10 $gL^{-1}$ concentration of adsorbent was used and mixed with the 25 ppm metal solution of Fe, Cu, Mn, Zn and As(III). That amount of adsorbent was taken based on the result from "effect of adsorption mass" experiment. 10 $gL^{-1}$ was the optimum adsorbent mass with almost 99% removal. The mixture of adsorbent and metal solution was then put onto a shaker at 100 rpm. A 5 ml of mixture was taken at several time differences such as 0.5 h, 1 h, 2 hrs, 4 hrs, 7 hrs, 9 hrs, 12 hrs, 24 hrs and 48 hrs. The mixture was filtered with 0.2 µm syringe filter and collected in plastic tube for ICP analysis.

### 4.5.4 Effect of initial solution concentration

This experiment is carried out with different initial metal solution concentrations. The initial concentration used here were 1 ppm, 5 ppm, 10 ppm, 25 ppm, 50 ppm, 75 ppm and 100 ppm.

Required amount of metal salts for each concentration were calculated and weighed for all metals (Fe, Cu, Mn, Zn and AsIII). The adsorbent dose was same for all (10 $gL^{-1}$) and temperature was room temperature. The weighed metals salts were dissolved in 10 ml ultrapure water in a 15 ml plastic tube. These mixtures were then put on a mechanical shaker at 100 rpm for 12 hours. Finally, mixtures were filtered with 0.2 µm syringe filter and collected in plastic tubes for ICP analysis.

### 4.5.5 Column experiment

Metal uptake by adsorbent during continuous flow was examined through column test. Micro-column (1.2 cm x 10 cm, pyrex glass) was used to conduct experiment with synthetic solution and natural water. They were fed into the column by a peristaltic pump (Watson Marlow 120S) at different flow rates of 2, 4, 6 and 8 ml $min^{-1}$. Effluent was collected after each 30 min interval and analysed with ICP-OES. Solid adsorbent was recovered after the completion of experiment, dried at 60$^{o}$C for 24 hours and analysed with TOF MS.

# 5. Results and Discussions

## 5.1 Synthesis of adsorbent

In RH material, presence of iron in the form of sulfate ($FeSO_4$) is a high possibility due to the presence of both iron and sulfide. In this case, the iron is present in the form of $Fe^{2+}$. Upon reaction with NaOH, a grey precipitate is formed in the beginning, which finally turns into dark brown due to oxidation at higher temperature and in presence of air. It is known from (Jolivet et al., 2004) that $Fe(OH)_2$ forms due to hydroxylation of $Fe^{2+}$ at pH>7. Hydroxylation of ferrous ions by the addition of NaOH solution generates poor highly hydrated phase, known as ferrihydrite. However, poor structural configuration makes ferrihydrite thermodynamically unstable. The transformation of ferrihydrite to different phases proceeds through different pathways based on the pH of the medium. At 5≤ pH ≤8, solubility of solid is very low and ferrihydrite transforms into haematite. At pH < 4 or pH > 8, the transformation undergoes a dissolution-crystallization process to produce goethite (α-FeOOH) (Misawa et al., 1974; Jolivet et al., 2004). This phenomenon is also shown in figure 4.

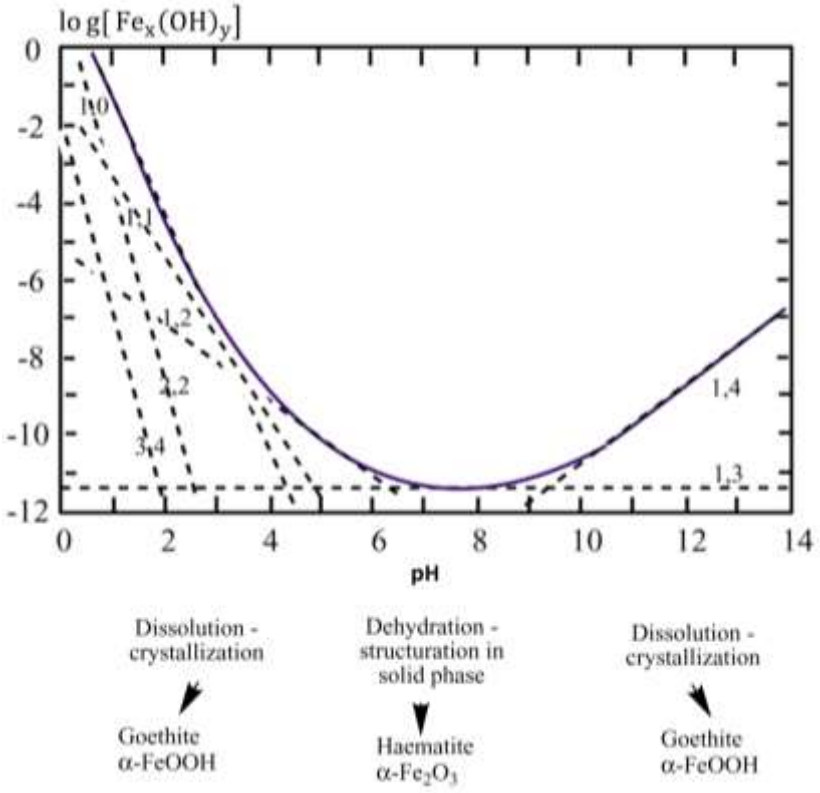


**Figure 5. Influence of pH on the solubility of iron and ferric (hydro) oxide crystal structure. Modified from** *(Jolivet et al., 2004)*

## 5.2 Characterization

### 5.2.1 BET

Table 2 details the surface area and pore characteristics for original RH and modified RH (RH2M) with various concentration of sodium hydroxide solution (1M, 2M and 4M). It clearly shows that increasing sodium hydroxide solution from 1M to 2M increases surface area considerably but further increase to 4M does not increase surface area at all. Pore diameter for RH2M is around 3 nm, which is similar to the pore sizes of magnetic iron oxide/mesoporous silica nanoparticles described by (Iakovleva et al., 2016 (under review)). RH 2M was further characterized as a potential adsorbent for mine water treatment.

**Table 2. Specific surface area and pore characteristics of unmodified and modified RH.** *(Iakovleva et al., 2016)*

| | Particle size | Specific surface area, $m^2\ g^{-1}$ | Pore volume $cm^3\ g^{-1}$ | Pore diameter nm |
|---|---|---|---|---|
| RH Original | 180 µm | 62.5 | - | - |
| RH 1M | 200 µm | 75 | - | - |
| RH 2M | 15-20 nm (20%)<br>200-250 nm (85%) | 950 | 0.3 | 3.2 |
| RH 4M | 15-20 nm (20%)<br>200-250 nm (85%) | 940 | 0.31 | 3.0 |

### 5.2.2 XRD

Figure 5 shows the XRD patterns for original RH and modified RH. From table 1, we can see the chemical composition of original RH, which tells us that the iron present in the material most probably be in the form of sulphate due to higher presence of Sulphur (17.6 %). Gypsum contained in the original RH can also be confirmed from XRD analysis in fig. Comparing two XRD patterns of original and modified RH clearly shows the modification that gives fundamentally new structure to RH2M. The diffraction peak at $45^0$ in RH2M is for the characteristic low crystalline/amorphous metallic iron (Yavuz et al., 2006). The characteristic peaks in RH2M at $21^0$, $33^0$, $42^0$ and $52^0$ are for the α-Fe(OOH), respectively (Varanada et al., 2002). So, presence of goethite nanoparticles can be confirmed.

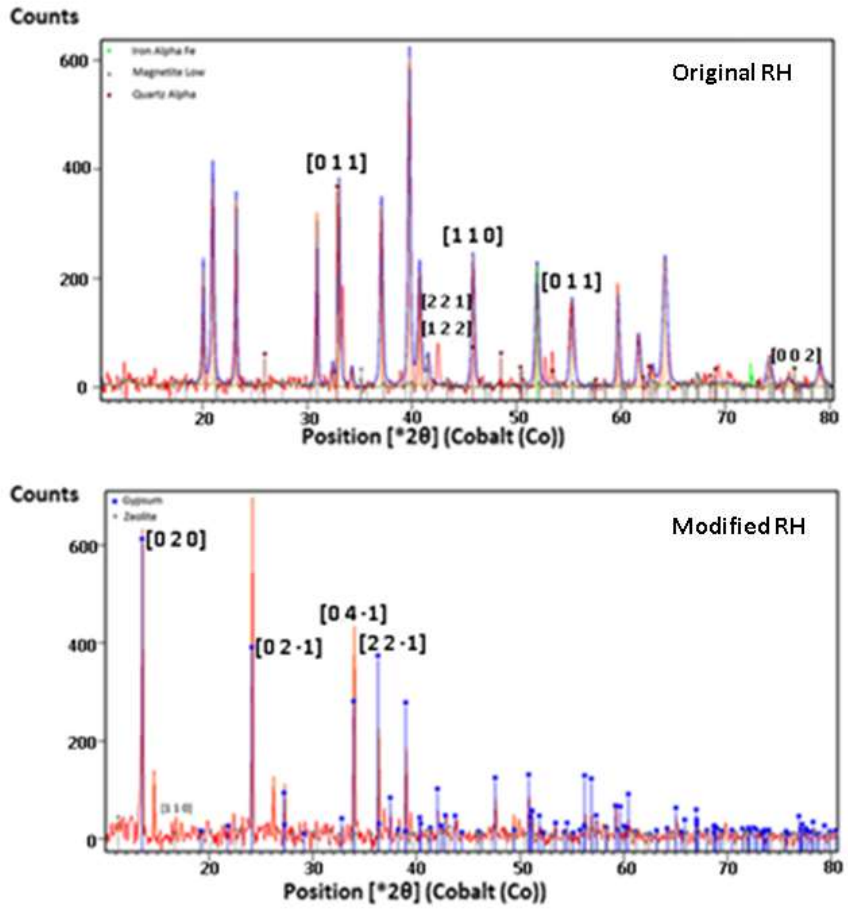


**Figure 6. XRD analysis for original and modified RH.**

### 5.2.3 FTIR

During alkaline treatment, the surface of RH was covered with hydroxyl groups in aqueous solution. The peaks at 3643 $cm^{-1}$ 2360 $cm^{-1}$ and 1418 $cm^{-1}$ are attributed to stretching vibrations for O-H, α-Si(OO) and α-Fe(OOH) respectively. This further supports the results from XRD. Table 3 shows the results from FTIR.

**Table 3. Vibrational bands of FTIR analysis for original and modified RH.**

| | Si-O-Si | Si-O-Si | Fe-OH | O-S-O | α-Fe(OOH) | H-O-H | α-Si(OO) | -OH | -OH |
|---|---|---|---|---|---|---|---|---|---|
| | 597 | 677 | 873 | 1003-1110 | 1418 | 1619-1682 | 2341-2360 | 3397-3495 | 3643 |
| RH 2M | | | + | + | + | | + | | + |
| RH | + | + | + | + | | + | | + | |

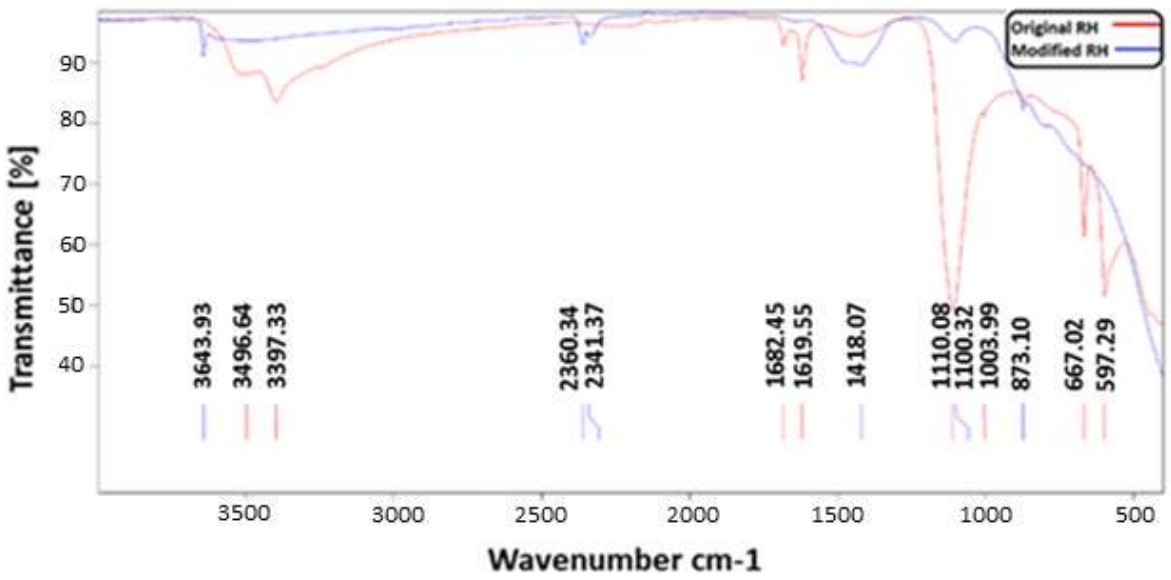


**Figure 7. FTIR analysis of original and modified RH.**

### 5.2.4 TEM

Figure 7 shows the TEM images for RH2M. Figures 7 a and b show the variation in size of nanoparticles from 15-20 nm and 200-250 nm and are spherical in shape. Around 75 % of the particles are close to 200 nm in size and almost 20 % are 20 nm in size. As we have seen the presence of silica or silicon dioxide from FTIR, the larger particles seen in TEM image correspond to magnetic mesoporous silica nanoparticles, while smaller particles to iron oxide/hydroxide nanoparticles (Iakovleva et al., 2016(under review)). Due to the strong magnetic properties of these particles, particles tend to attract each other forming large agglomerates.

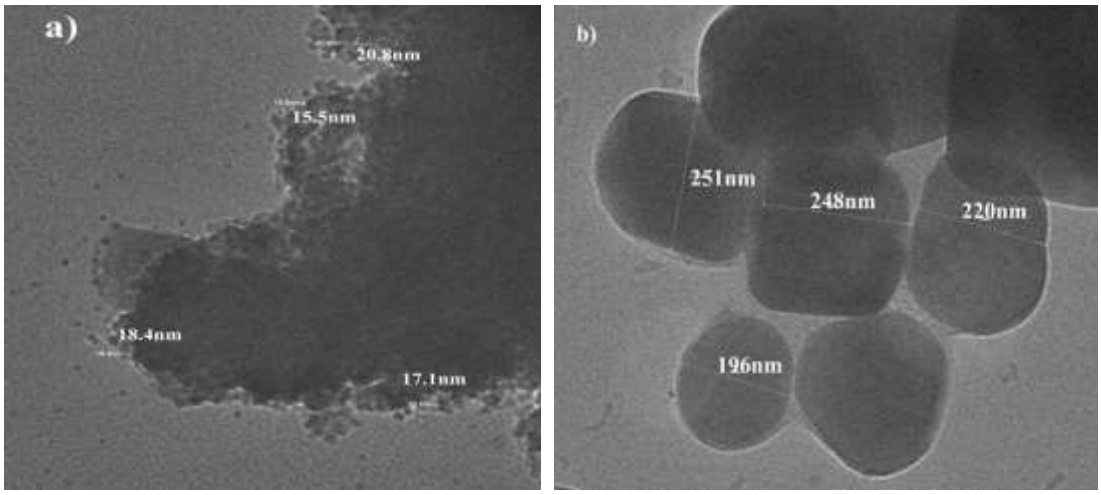


**Figure 8. TEM picture for original and modified RH.** *(Iakovleva et al., 2016)*

## 5.1. Experimental results

Figure 8 below shows the effect of pH on the adsorption of As, Mn, Zn, Fe and Cu at different pH ranges. Removal percentage is almost 100 % for all the metals except As(III). For As(III), it seems that adsorption with RH2M adsorbent is more favorable at pH below 7 with exception to pH 5. The low removal percentage at pH 5 can be attributed to the formation of positive ions on the surface of adsorbent, which can further be confirmed by the zeta potential values shown in figure 9.

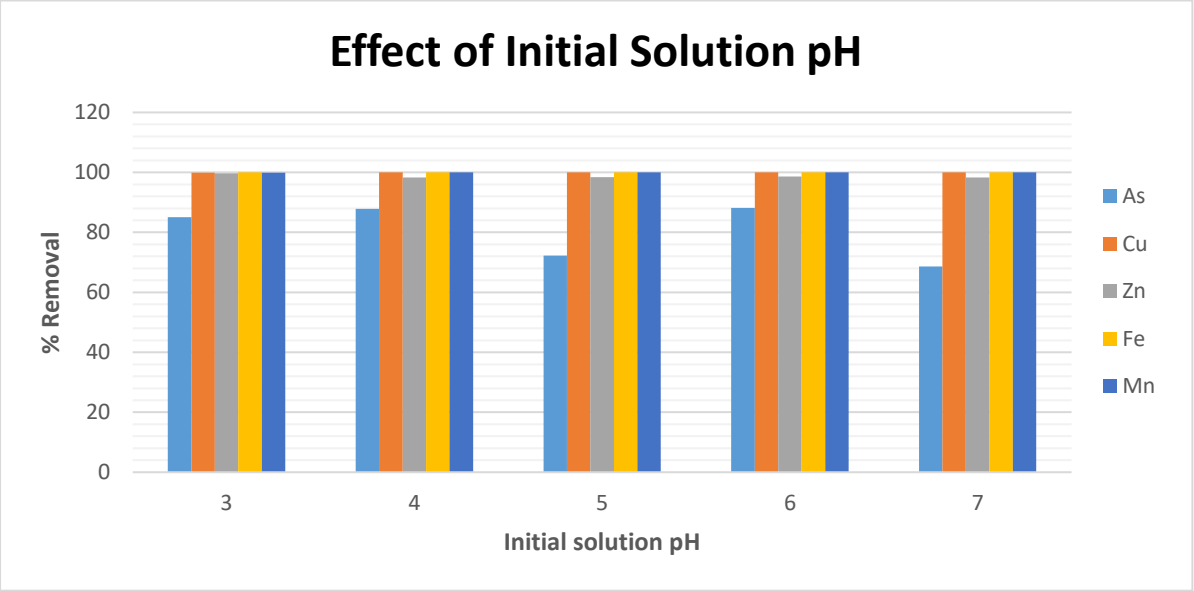


**Figure 9. Removal efficiency of RH2M adsorbent at different initial solution pH.**

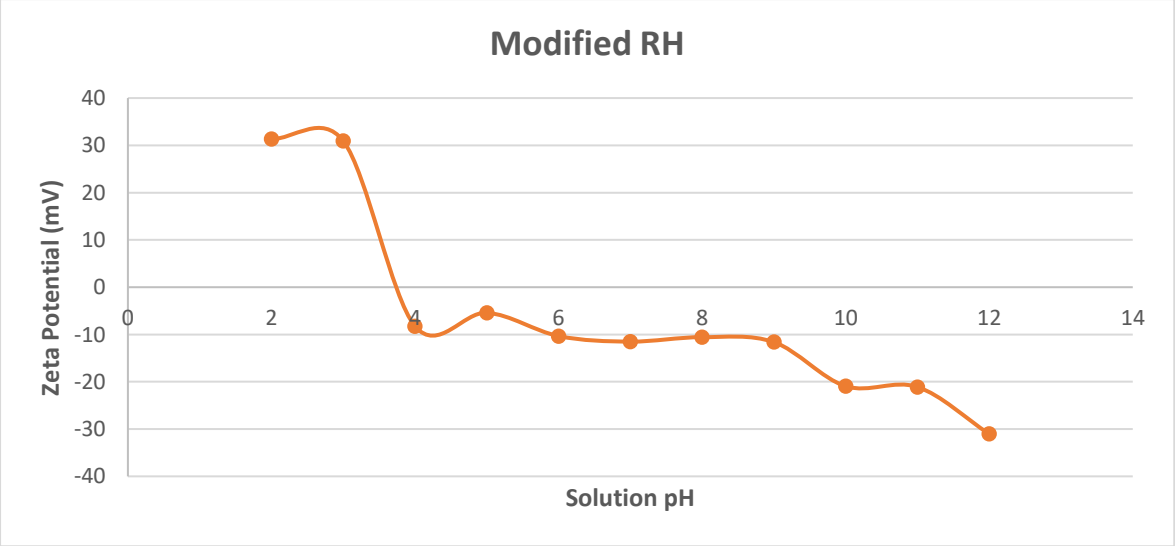


**Figure9. Zeta potential values at different pH for RH2M.**

Figure 10 below shows various ionic formations of different metals at different pH. Final pH after adsorption experiment for all the metal ion solutions was between pH 11 – 12. This can be attributed to the highly basic nature of adsorbent. Measurement of redox potential of final arsenic solution puts the final arsenic formation to $AsO_4^{3-}$, which tells us that arsenic III has been converted to arsenic V at pH beyond 12.

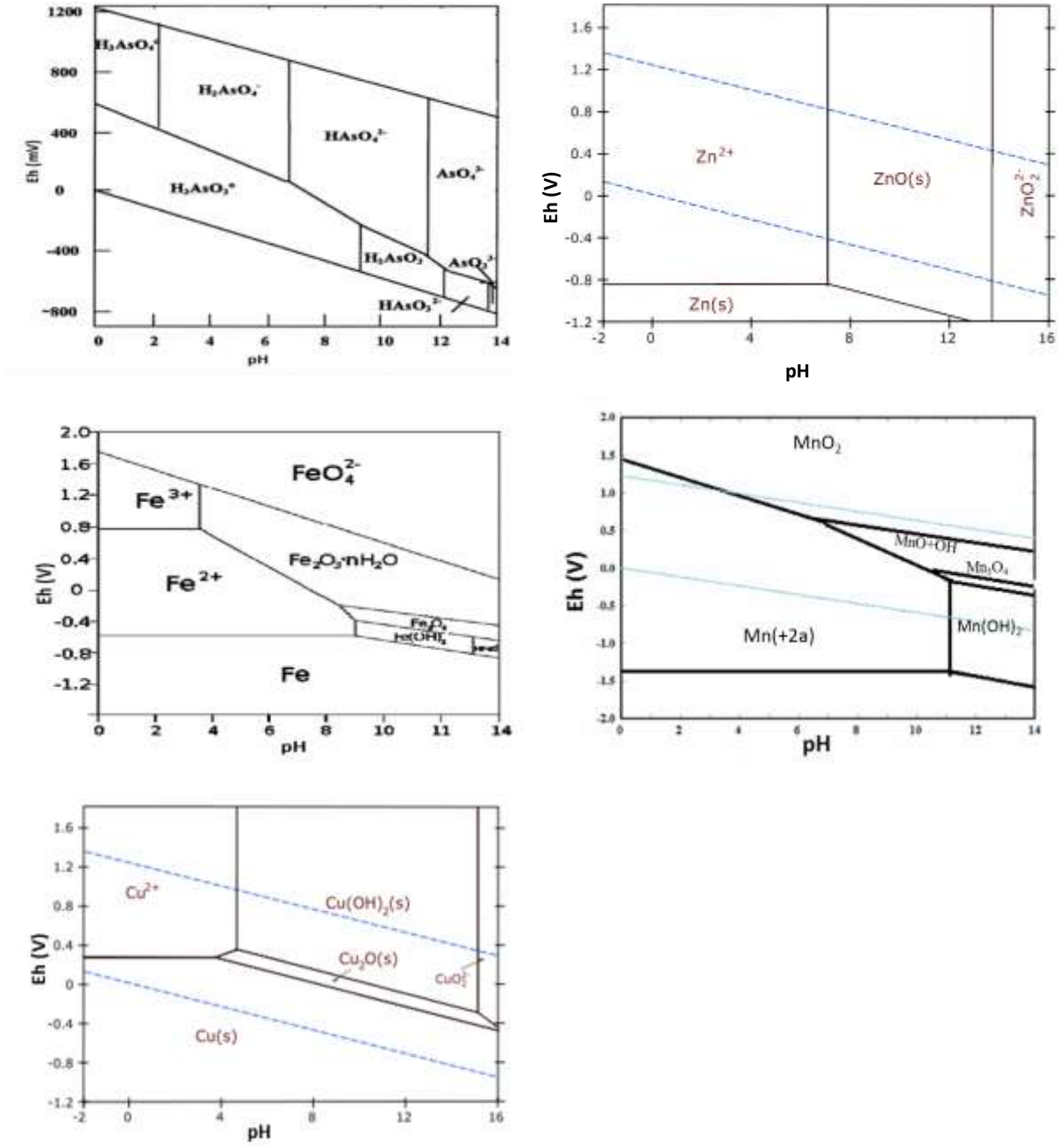


**Figure 10. Redox potential ($E_H$)-pH diagram for aqueous elemental species (Fe, Mn, Cu, Zn and As) during dissolution. (Modified from** *(Akter et al., 2005) (Massaro, 2002)***)**

The higher adsorption of Zn, Mn, Cu and Fe is related to their positive valence states at the pH range between 3 and 7. In the pH range of 11 – 12, all the other metals except As precipitate as hydroxide.

Figure 11 shows the removal efficiency with various adsorbent doses. This is a crucial variable in the design of adsorption processes to determine the capacity for any given component. The metal uptake capacity increased with increased adsorbent dose as expected. At constant concentration of metal ions in a solution, increasing adsorbent dose increases the adsorption of metal ions due to the availability of more free adsorption sites for metal ions. Moreover, all the adsorption sites are not occupied by metal ions so, the adsorbent remains unsaturated and further increasing the adsorbent dose means increasing the adsorbent sites, which will not be used at all.

It can be seen that adsorption for Fe, Mn, and Cu were at the same level i.e. 100% even with smaller amount of adsorbent. For As(III), plot shows that optimum adsorbent dose for removal is around 5 -10 $gL^{-1}$, after which there is no significant increase in adsorption. For Zn, similar pattern presents except that 88% of zinc is removed already at 0.5 $gL^{-1}$ so the amount of adsorbent dose depends on the removal demand.

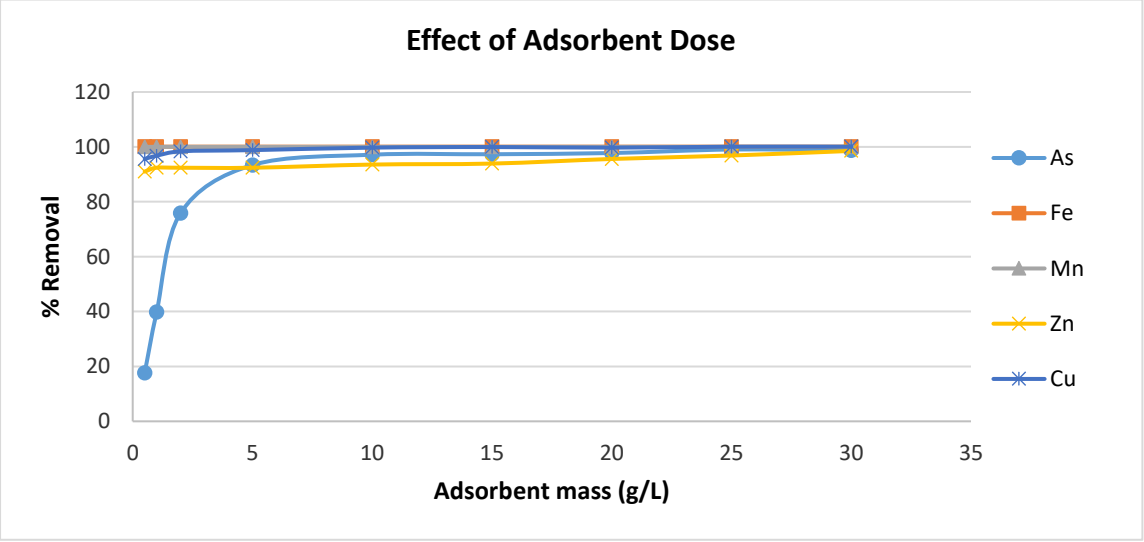


**Figure 10. Effect of adsorbent dose on adsorption of different metal ions with 25 ppm concentration for each and at pH6**.

Figure 12 shows the effect of initial solution concentration for metals. Effect of initial solution concentration was investigated for 1 ppm, 5 ppm, 10 ppm, 25 ppm, 50 ppm, 75 ppm and 100 ppm at room temperature. Initial metal concentration does have effect as can be seen from the plots however, arsenic and zinc have lower removal efficiency at the lower initial solution

concentration. The metal uptake is increased along with increase metal concentration, which means there is still plenty of adsorption sites available for metal ions and ratio of adsorption sites to metal ions is quite high. This can also be looked from the other side. This observation also explains that adsorption of metal ions may involve the diffusion phenomena whereby, metal ions tend to move from high concentrations to low concentrations. This driving force can increase mass transfer between aqueous metal solution and solid adsorbent. Steeper concentration gradient can intensify the movement of metal ions. Therefore, increasing metal ions concentration increased the removal efficiency.

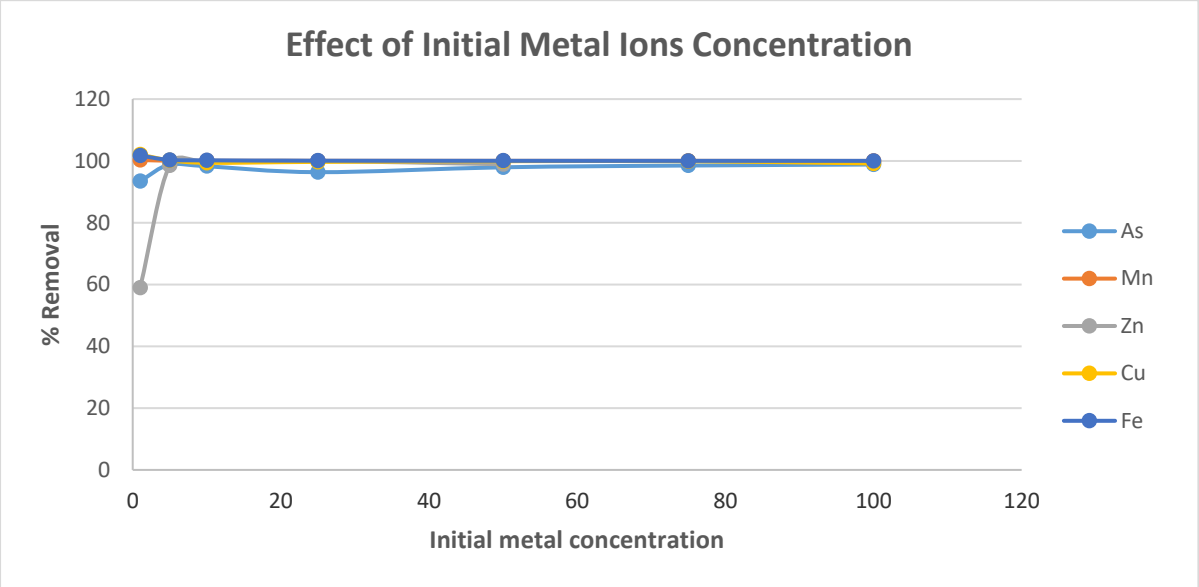


**Figure 11. Effect of initial metal concentration on adsorption of different metals**.

## 5.2 kinetics Study

Below in figure 13, we can see the effect of contact time on the adsorption of metals. The adsorption process seems quite fast with 90 – 100 % removal for all metals within 30 minutes. For Fe, Cu and Mn, the process reaches equilibrium already after 30 minutes, which is more or less similar for Zinc and Arsenic. This is a very impressing, when used in the mine site low retention time in the adsorption column is a benefit as more polluted water can be treated at a reasonable timeframe. Figure 13 suggests that adsorption occurs very rapidly during the initial stage on the external surface of adsorbent accompanied by slower internal diffusion, which can be the rate-determining step. The faster adsorption in the initial stage can be described by the availability of large number of adsorption sites on the surface but with time lapse these sites fill up and remaining sites are difficult to be occupied. The reason behind this is due to the

repulsive force between the adsorbates present in adsorbent and in bulk solution, which increases the time to reach equilibrium.

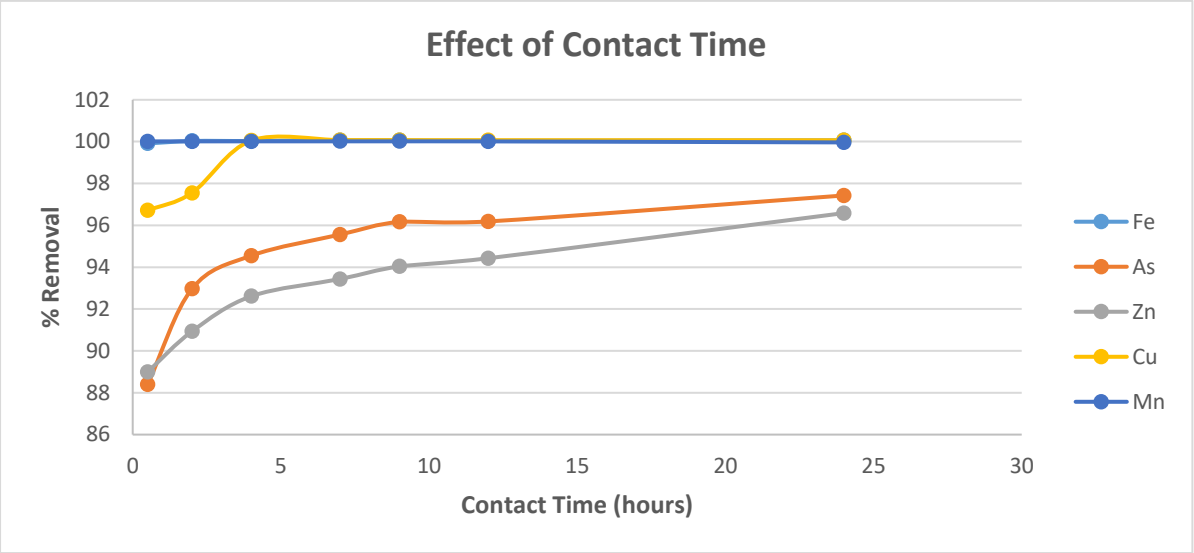


**Figure 12. Plot of removal percentage versus contact time (hours) for metal ions using RH2M adsorbent.**

The sorption kinetics was investigated in order to determine the adsorption rates for the metal ions. Two adsorption kinetic models, namely, pseudo first order and pseudo second order were studied. The adsorption for Cu, Fe and Mn was so fast (<30 min) and was not appropriate for kinetic study so another set of adsorption experiment was performed particularly for these metal ions. Samples were taken and analyzed at an interval of 5 minutes as shown in figure 14. The adsorbent dose, initial metal ion concentration and temperature were all kept same.

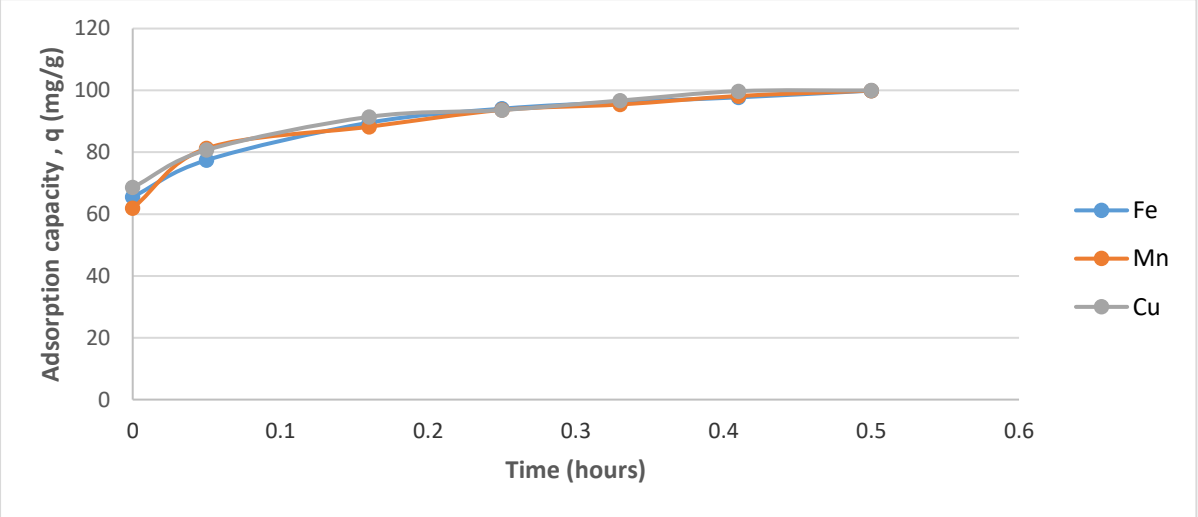


**Figure 13. Adsorption over different contact time.**

Linear and non-linear fitting results are shown in table 4 and figures 15 to 19. In pseudo first order linear fitting, two $q_e$values are used; one directly from the adsorption values and other from the linear plot. Therefore, the $q_e$ value is not reliable. However, in pseudo second order only single $q_e$ is predicted from linear fitting. This can also be seen through correlation coefficient $r^2$ values. Higher correlation coefficient $r^2$ value suggests that metal ions followed pseudo-second order kinetics and they were adsorbed onto RH2M adsorbent via chemisorption. Valence forces might have been involved in sharing electrons between adsorbent and adsorbate inducing chemisorption. In addition to that, for second order model experimental $q_{e\ exp}$ values agree well with the theoretical $q_{e\ cal}$ values for all absorbate studied.

**Table 4. Linear Pseudo-first order and pseudo-second order kinetic model parameters. exp refers to experimental value and cal refers to calculated value. The initial concentration of all metal ions was 25 $mgL^{-1}$, adsorbent mass 0.1 g, time (5-1440) min, 298.15 K and 101kPa.**

| | | Pseudo-first order | | | Pseudo-second order | | |
|---|---|---|---|---|---|---|---|
| Metal Ions | $q_{e\ exp}$ $mg\ g^{-1}$ | $q_{e\ cal}$ $mg\ g^{-1}$ | K | $r^2$ | $q_{e\ cal}$ $mg\ g^{-1}$ | K | $r^2$ |
| As | 19.87 | 2.5 | 0.076 | 0.20 | 20.2 | 0.57 | 0.99 |
| Zn | 20.02 | 1.44 | 0.041 | 0.13 | 19.6 | 0.007 | 1 |
| Mn | 24.97 | 37.15 | 2,37 | 0,50 | 26.04 | 0.98 | 0.99 |
| Fe | 24.98 | 34.53 | 2.31 | 0.50 | 25.97 | 0.98 | 0.99 |
| Cu | 24.99 | 18.57 | 2.6 | 0.26 | 25.90 | 1.24 | 0.99 |

Table 5 shows the comparison between $q_e$ values calculated from both linear and non-linear equations. Usually, non-linear model is better because it does not require any assumptions and model can be used directly without linearization so it provides better approximation and more reliable parameter values. The $q_e$ values from non-linear models are quite close to the experimental values with pseudo-second order being the better one. This can further be seen from the plots in figures 15 to 19.

**Table 5. Comparison between linear and non-linear fitting of pseudo first order and pseudo second order models**.

| | | Pseudo-first order | | Pseudo-second order | |
|---|---|---|---|---|---|
| | | Linear | Non-linear | Linear | Non-linear |
| Metal Ions | $q_{e\ exp}$ mg $g^{-1}$ | $q_{e\ cal}$ mg $g^{-1}$ | $q_{e\ cal}$ mg $g^{-1}$ | $q_{e\ cal}$ mg $g^{-1}$ | $q_{e\ cal}$ mg $g^{-1}$ |
| As | 19.87 | 2.5 | 18,46 | 20.2 | 19,55 |
| Zn | 20.02 | 1.44 | 18,48 | 19.6 | 19,02 |
| Mn | 24.97 | 37.15 | 23,53 | 26.04 | 25,79 |
| Fe | 24.98 | 34.53 | 23,41 | 25.97 | 25,53 |
| Cu | 24.99 | 18.57 | 23.62 | 25.90 | 25.51 |

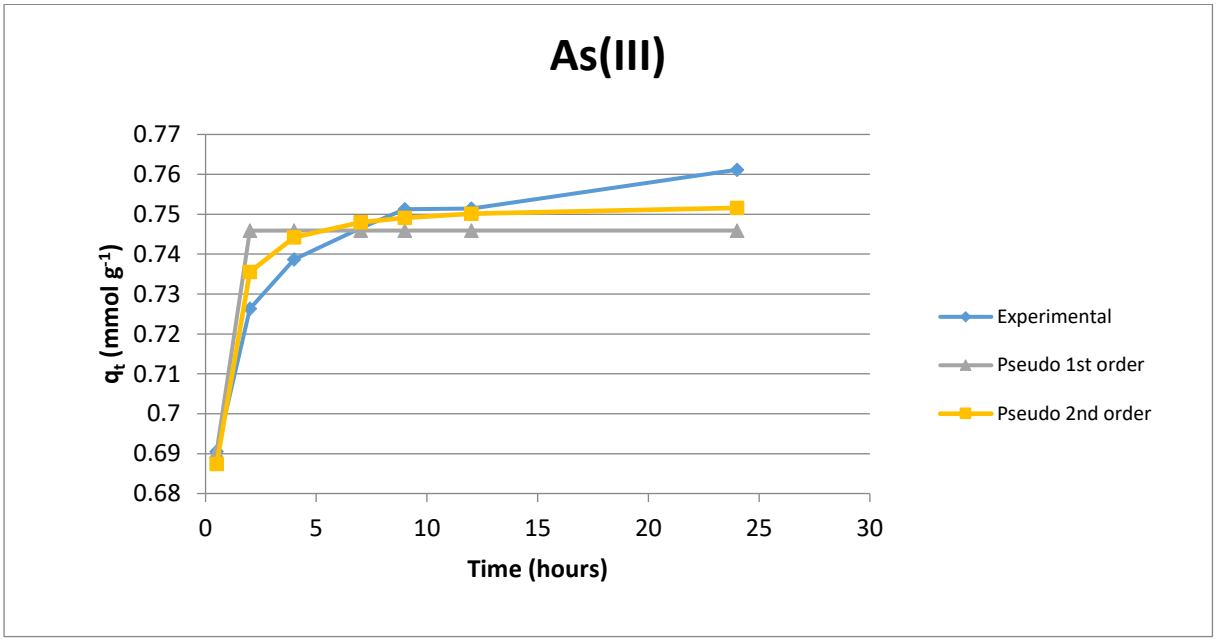


**Figure 14. Plot for time dependent sorption capacity ($q_t$, mg $g^{-1}$) of As(III).**

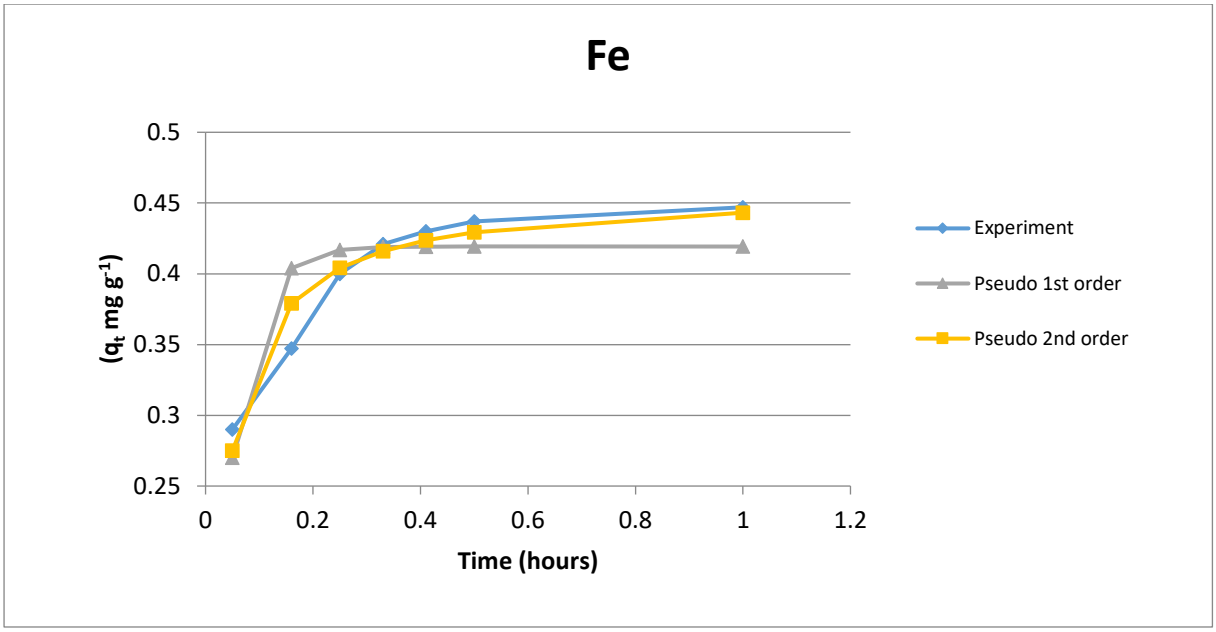


**Figure 15. Plot for time dependent sorption capacity ($q_t$, mg $g^{-1}$) of Fe.**

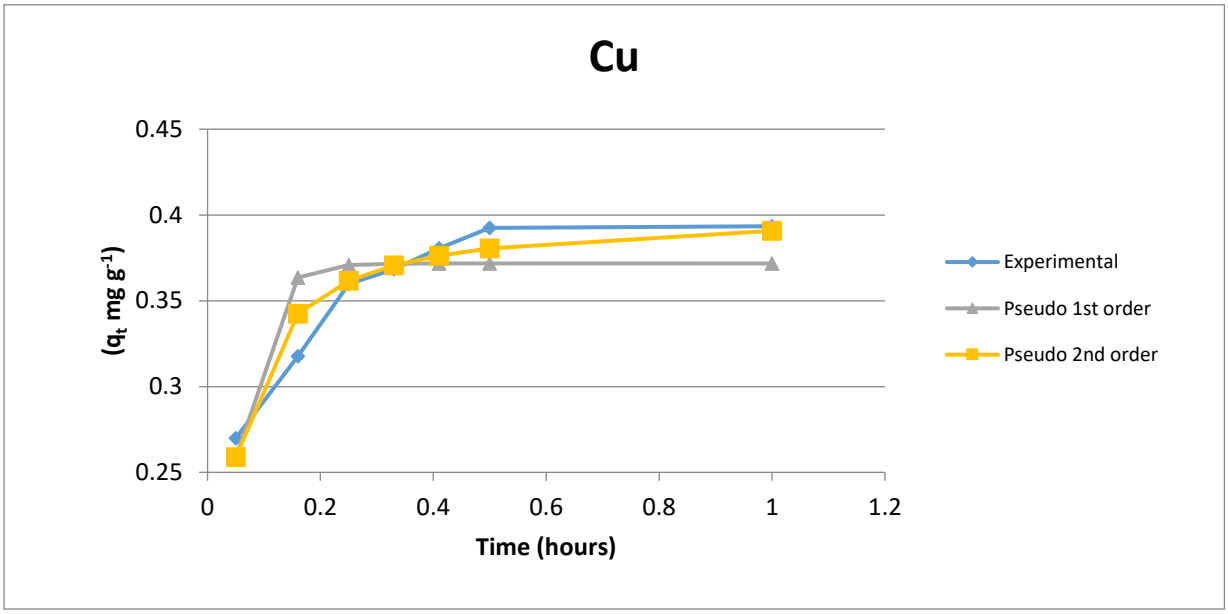


**Figure 16. Plot for time dependent sorption capacity ($q_t$, mg $g^{-1}$) of Cu.**

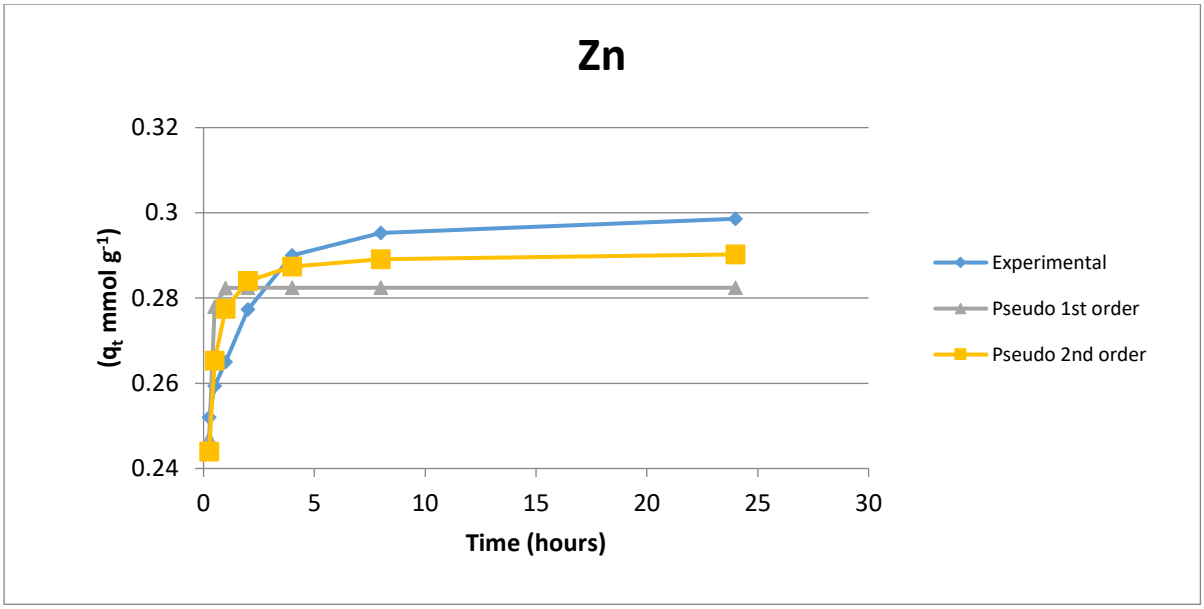


**Figure 17. Plot for time dependent sorption capacity ($q_t$, mg $g^{-1}$) of Zn.**

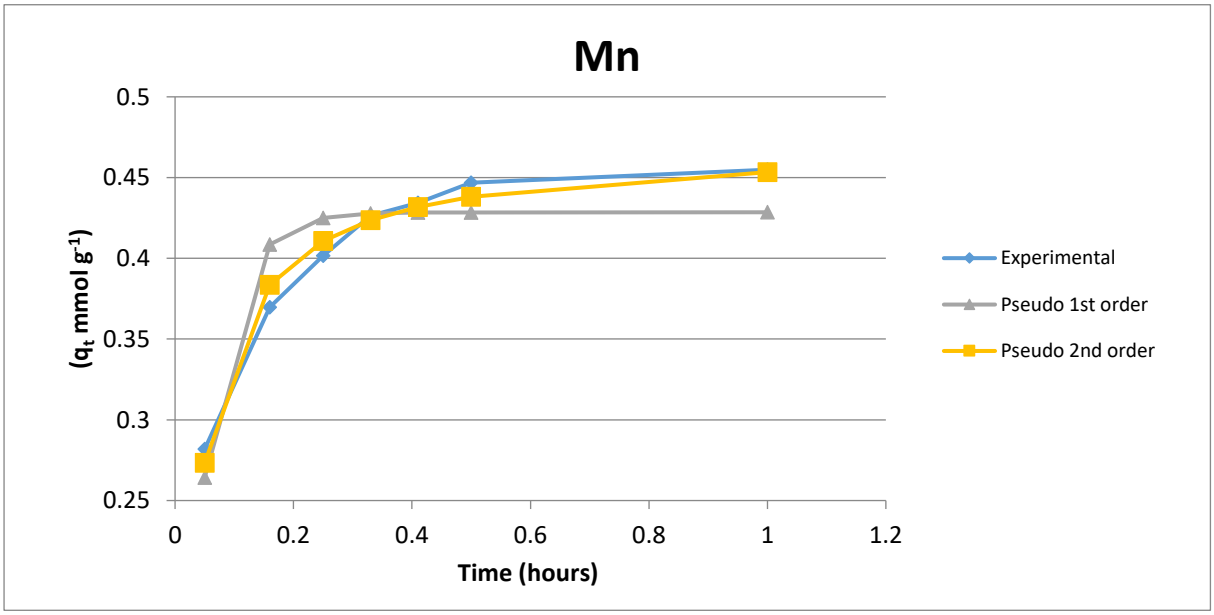


**Figure 18. Plot for time dependent sorption capacity ($q_t$, mg $g^{-1}$) of Mn.**

## 5.3. Isotherm Studies

### 5.3.1. Arsenic (III)

Adsorption studies was further done plotting isotherm models for each metal ions (As(III), Cu, Zn, Mn and Fe). For this work, only Langmuir and Freundlich isotherm models were compared as they are the most famous isotherm models and also on the basis of previous similar studies done by various authors.

Below in figure 20 and 21, we can see the Langmuir and Freundlich isotherm models for As(III). It can be seen that for As, Freundlich model is a best fit based on the $R^2$ value. Below in table 6, we can see the maximum adsorption capacity $q_m$ as 1.17 mmol $g^{-1}$ and other isotherm values for both models.

**Table 6. Isotherm parameters at equilibrium for As adsorption on RH2M.**

| | Langmuir | | Freundlich | |
|---|---|---|---|---|
| | $q_m$ mmol $g^{-1}$ | $K_L$ L $mg^{-1}$ | n | $K_F$ mg/g |
| Experimental | 1.04 | 0.030 | 1.61 | 3.5 |
| Model | 1.17 | 0.025 | 1.93 | 5.8 |

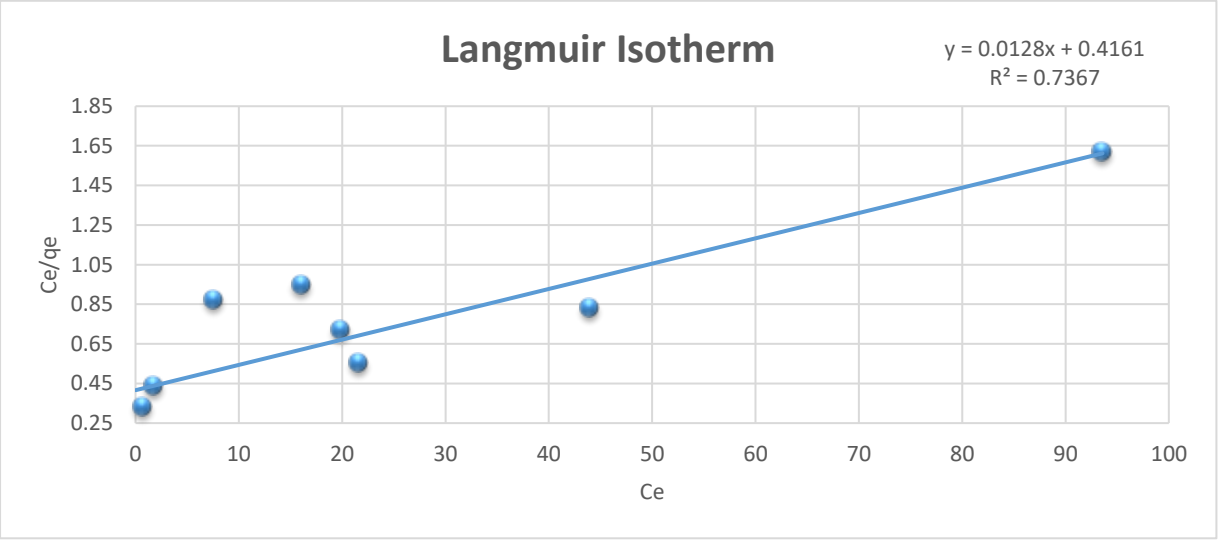


**Figure 19. Langmuir isotherm fitting for As(III).**

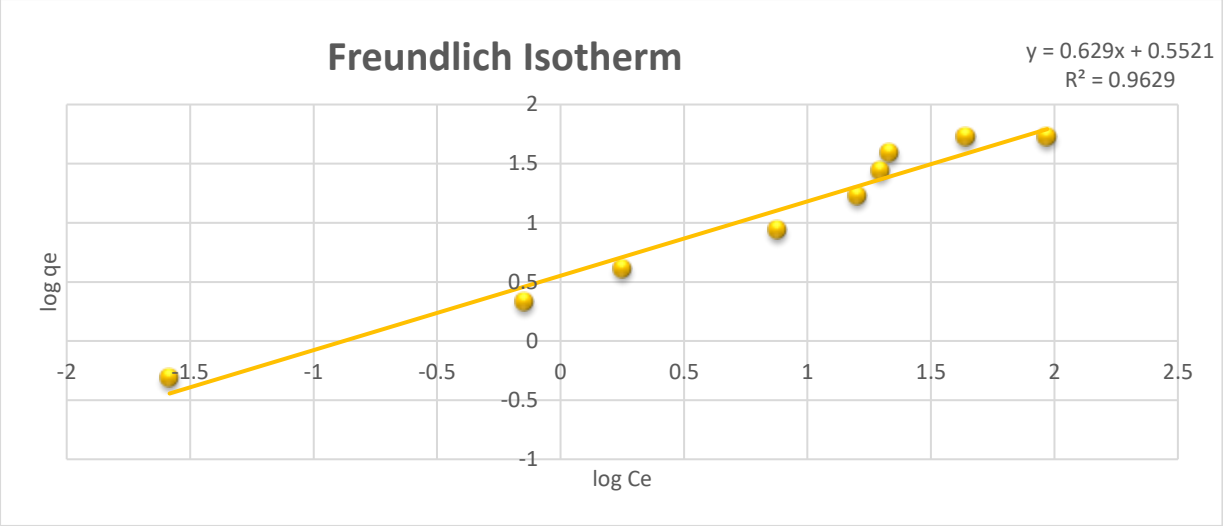


**Figure 20. Freundlich isotherm fitting for As(III).**

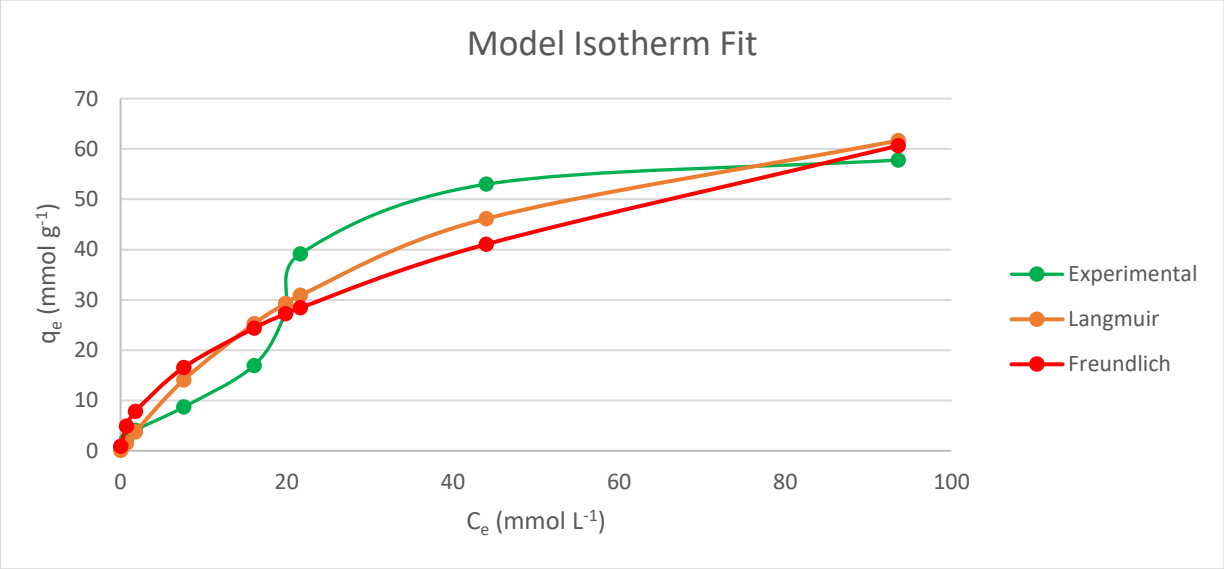


**Figure 21. Plots of qe(mg $g^{-1}$) versus Ce (mg $L^{-1}$) for As(III) adsorption.**

The Langmuir maximum adsorption capacity ($q_m$) is not correct in the case of As(III) because it follows the Freundlich isotherm model. Therefore, to determine maximum adsorption capacity, it is necessary to operate with constant initial As(III) ion concentration ($C_i$) and variable weights of adsorbent (Naffrechoux & Hamdaouia, 2007). Therefore, logarithm of $q_m$ ($\ln q_m$) will be the extrapolated value of lnq for $C=C_i$. The Freundlich equation according to (Hasley, 1952) will be:

$$k_f = \frac{q_m}{{C_i}^{1/n}} \quad (3)$$

Where, $C_i$ is the initial concentration of the As(III) ions in the solution (mg $L^{-1}$) and $q_m$ is the Freundlich maximum adsorption capacity (mg $g^{-1}$).

**Table 7. Maximum adsorption capacity of As(III) with RH2M based on Freundlich isotherm model.**

| Experimental | | | Calculated | | |
|---|---|---|---|---|---|
| n | $K_F$ | $q_m$ mmol $g^{-1}$ | n | $K_F$ | $q_m$ mmol $g^{-1}$ |
| 1.63 | 9.39 | 1.38 | 2.25 | 14.17 | 1.07 |

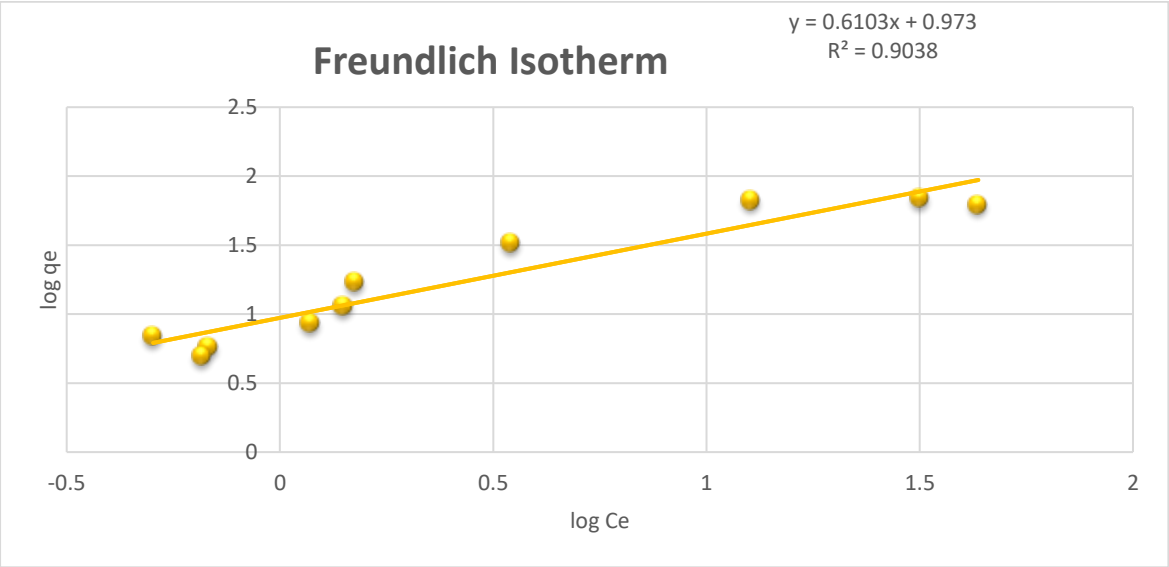


**Figure 22. Freundlich isotherm for As(III) with constant initial concentration (50 mg $L^{-1}$) and variable adsorbent mass**.

### 5.3.2. Iron

In the case of Fe, the adsorption property is well described by both isotherm model, however Langmuir model is the most favourable one. Therefore, for Fe as described by Langmuir, there is a monolayer adsorption. The experimental and calculated maximum adsorption capacity $q_m$ for Fe was 12.79 mmol $g^{-1}$ and 13.51 mmol $g^{-1}$.

**Table 8. Isotherm parameters at equilibrium for Fe adsorption on RH2M**.

| | Langmuir | | Freundlich | |
|---|---|---|---|---|
| | $Q_m$ mmol $g^{-1}$ | $K_L$ | n | $K_F$ |
| Experimental | 12.79 | 0.070 | 2.86 | 108.86 |
| Model | 13.51 | 0.039 | 3.08 | 122.38 |

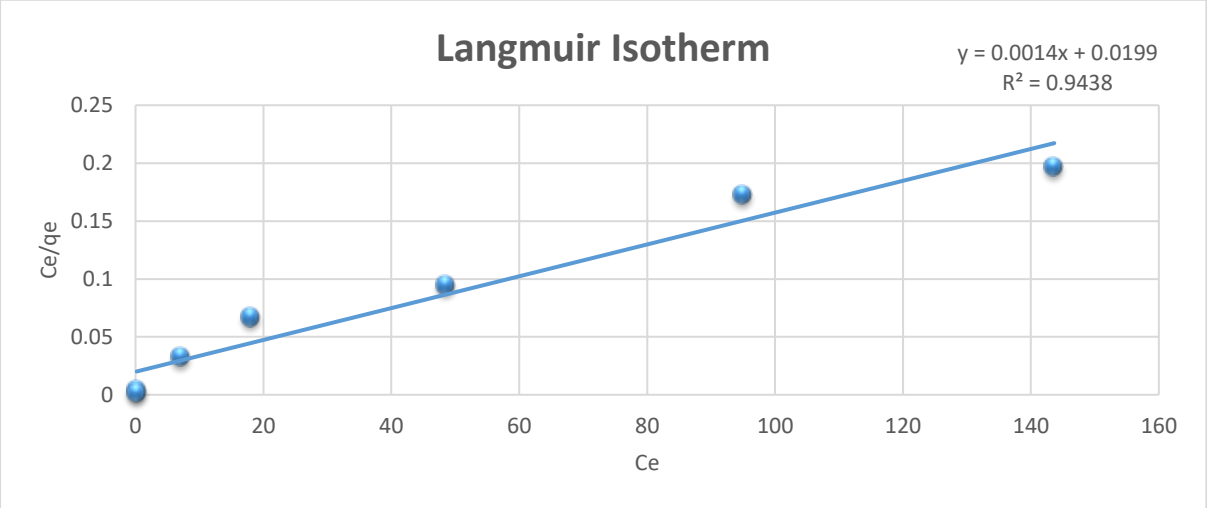


**Figure 23. Langmuir isotherm fitting for Fe.**

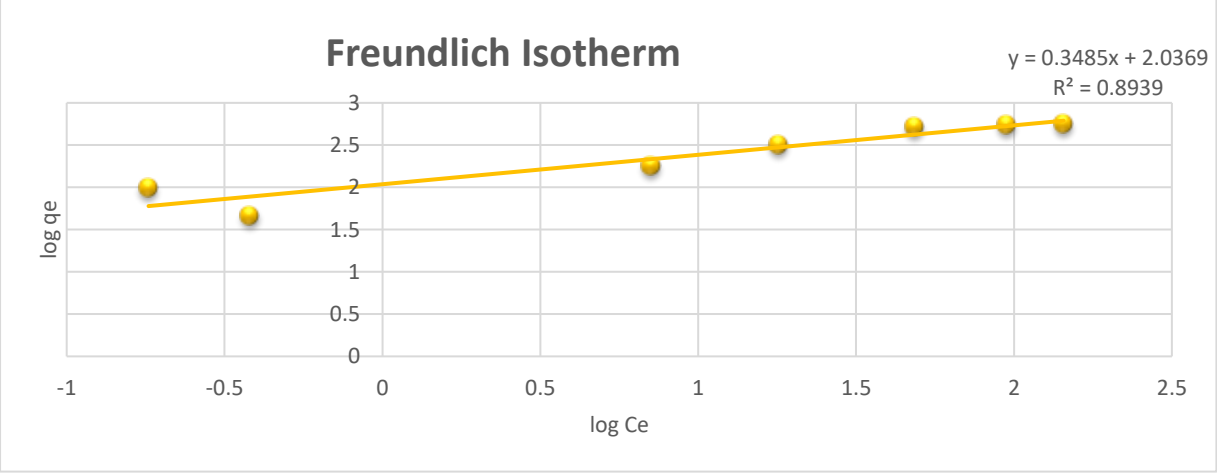


**Figure 24. Freundlich isotherm fitting for Fe.**

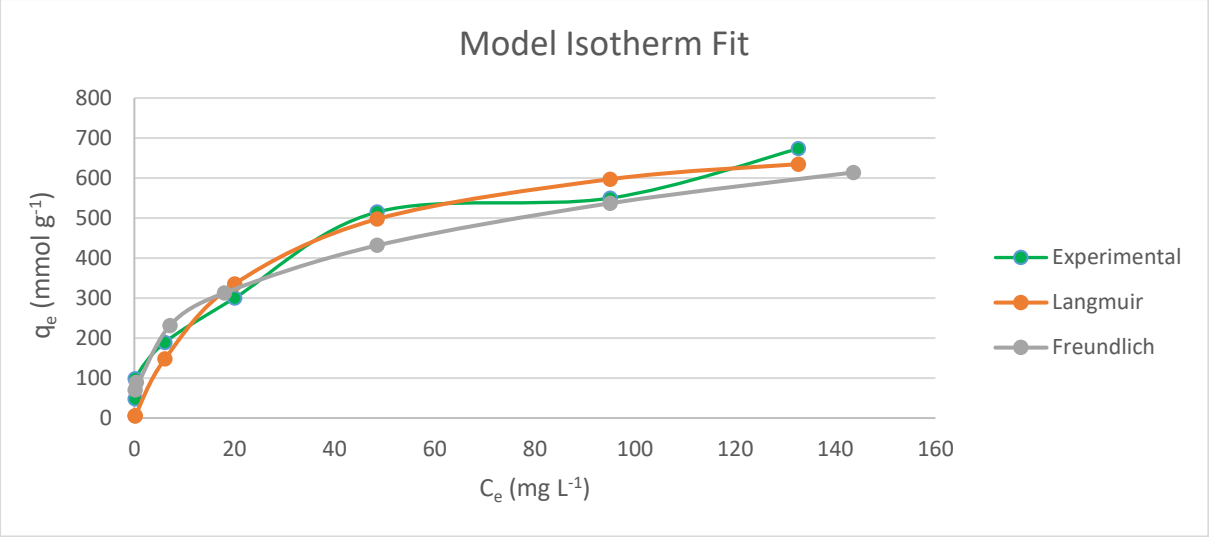


**Figure 25. Plots of qe (mg $g^{-1}$) versus Ce (mg $L^{-1}$) for Fe adsorption isotherm**.

### 5.3.3. Copper

For Copper, the adsorption is also monolayer as Langmuir isotherm is best suited with $R^2$ value of 0.98 compared to Freundlich with $R^2$ value of 0.91. The maximum adsorption capacity is higher compared to Fe and As as shown in table 9. The experimental and calculated maximum adsorption capacity $q_m$ for Copper ions were 15.73 mmol $g^{-1}$ and 14.23 mmol $g^{-1}$ respectively. In previous adsorption results, Cu was removed rapidly even at high concentrations from the solution and also required less amount of adsorbent, which further justifies the higher adsorption capacity.

**Table 9. Isotherm parameters at equilibrium for Cu adsorption on RH2M.**

| | Langmuir | | Freundlich | |
|---|---|---|---|---|
| | $q_m$ mmol $g^{-1}$ | $K_L$ | n | $K_F$ |
| Experimental | 15.73 | 0.21 | 2.48 | 181.55 |
| Model | 14.23 | 0.32 | 3.32 | 248.7 |

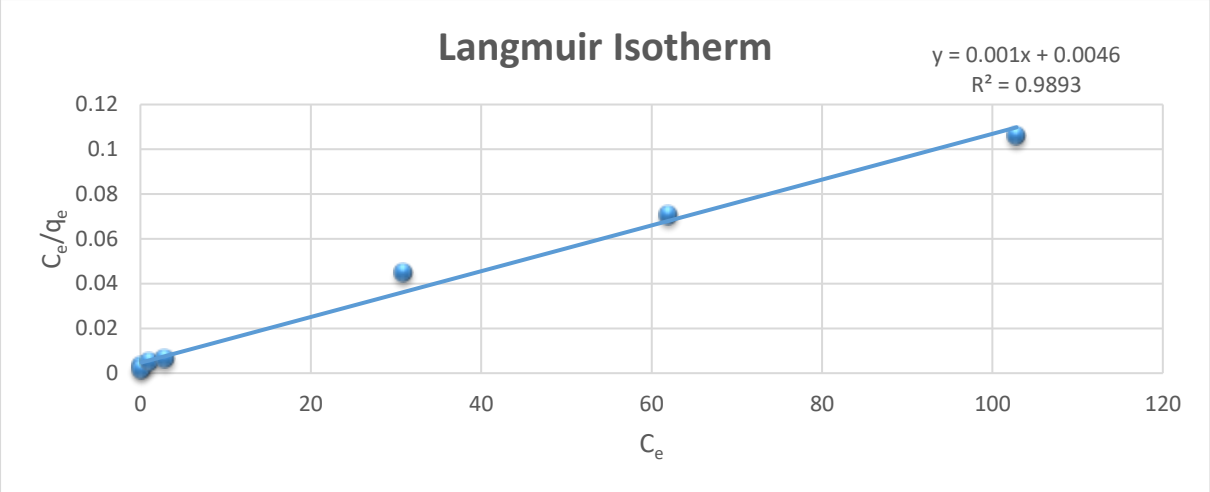


**Figure 26. Langmuir isotherm fitting for Cu.**

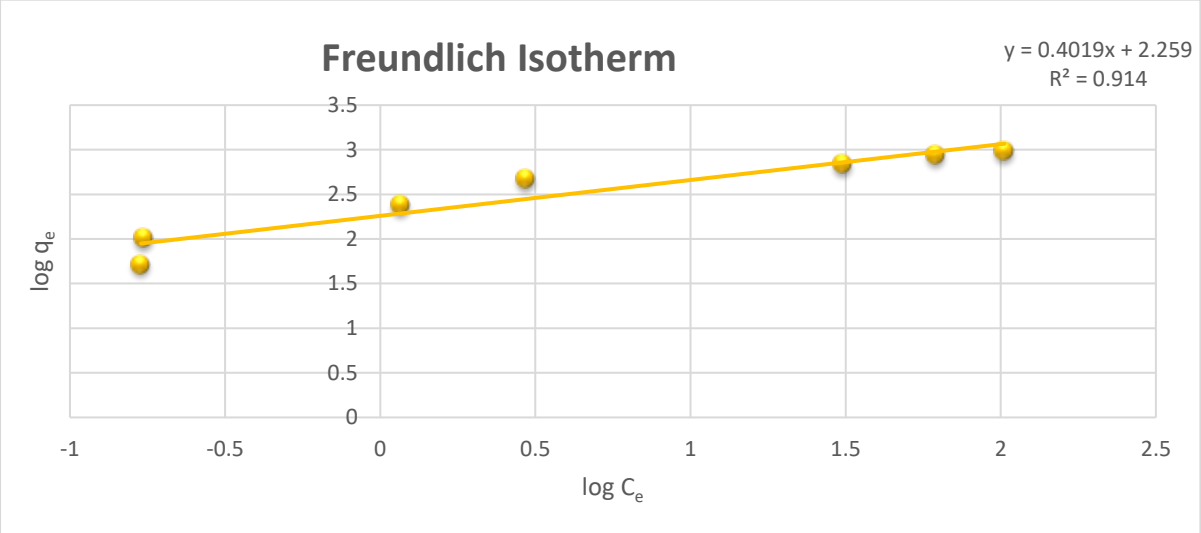


**Figure 27. Freundlich isotherm fitting for Cu.**

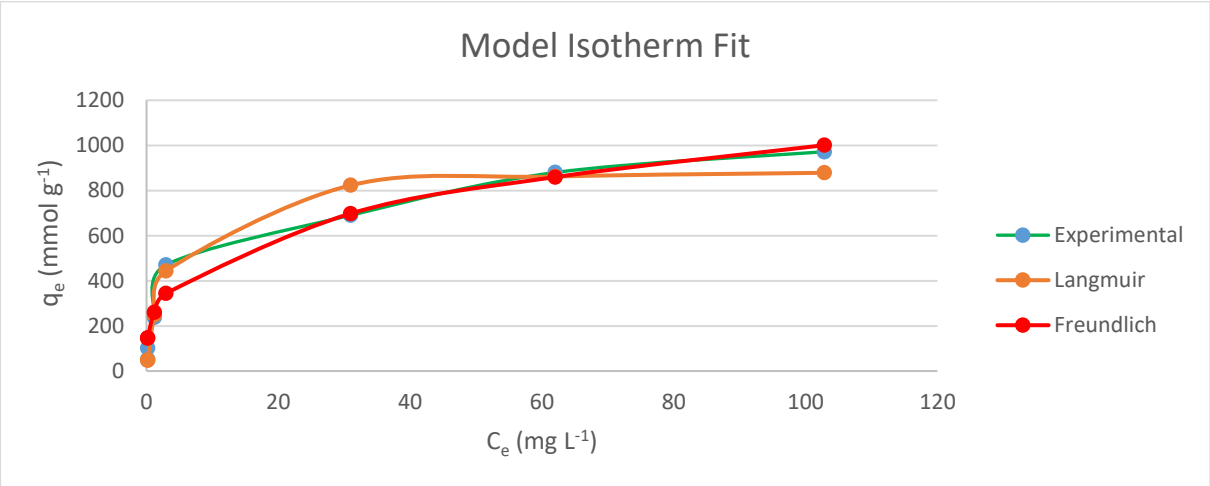


**Figure 28. Plots of qe(mg $g^{-1}$) versus Ce (mg $L^{-1}$) for Cu adsorption isotherm.**

### 5.3.4. Zinc

In the case of Zn, there is a monolayer adsorption as described by Langmuir model. The best fit isotherm model for Zn is Langmuir based on the $r^2$ value. However, Freundlich model is also quite close with only little difference. The experimental and calculated maximum adsorption capacity of RH2M adsorbent towards Zn given by Langmuir is 10.92 mmol $g^{-1}$ and 16.48 mmol $g^{-1}$ respectively.

**Table 10. Isotherm parameters at equilibrium for Zn adsorption on RH2M.**

| | Langmuir | | Freundlich | |
|---|---|---|---|---|
| | $q_m$ (mmol/g) | $K_L$ | n | $K_F$ |
| Experimental | 10.92 | 0.104 | 2.79 | 135.51 |
| Model | 16.48 | 0.028 | 2.01 | 85.58 |

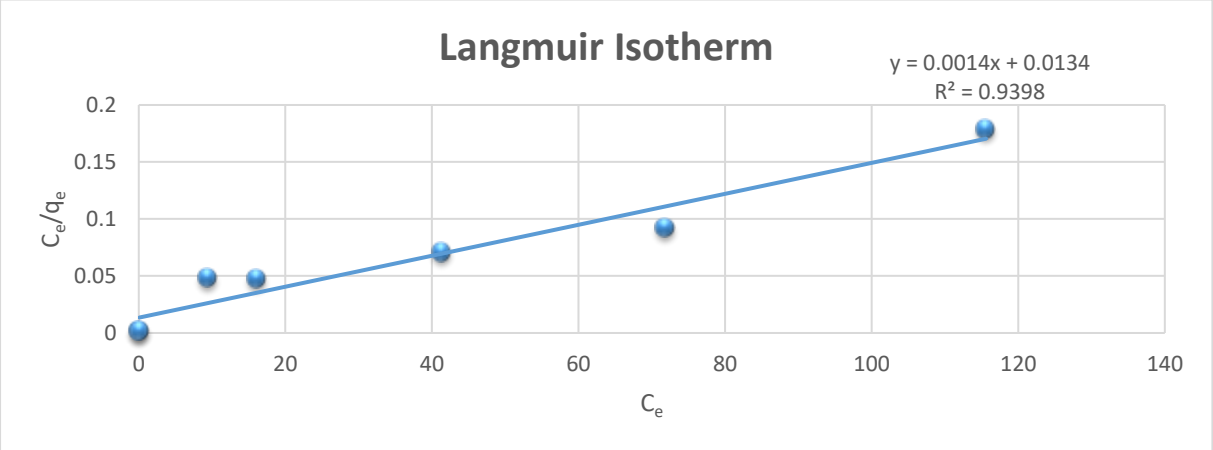


**Figure 29. Langmuir isotherm fitting for Zn.**

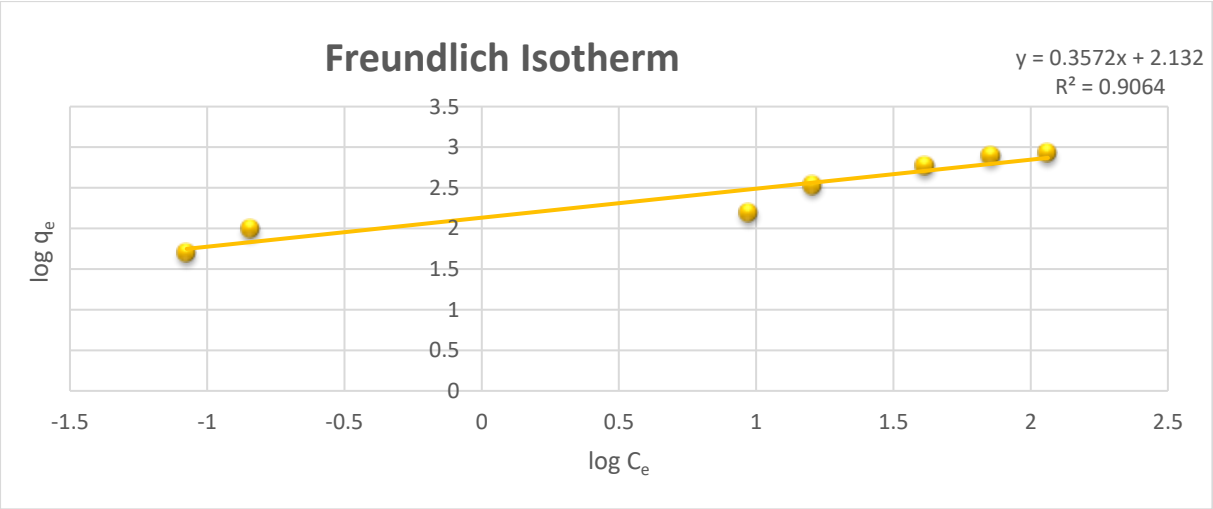


**Figure 30. Freundlich isotherm fitting for Zn.**

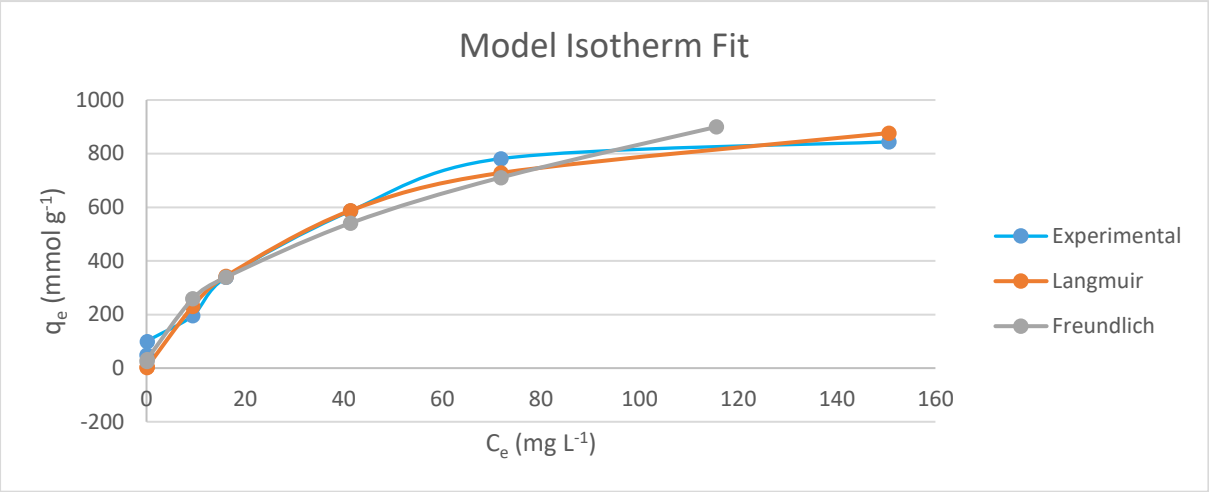


**Figure 31. Plots of qe(mg $g^{-1}$) versus Ce (mg $L^{-1}$) for Zn adsorption isotherm.**

### 5.3.5. Manganese

The R-value shown in table 11 indicates that the experimental results for Mn were best described by the Freundlich model. That means there is also multilayer deposition of Mn ions on the surface of RH2M. The experimental and calculated maximum adsorption capacity as given by Langmuir equation is 17.87 mmol $g^{-1}$ and 23.73 mmol $g^{-1}$ respectively.

**Table 11. Isotherm parameters at equilibrium for Mn adsorption on RH2M.**

| | Langmuir | | Freundlich | |
|---|---|---|---|---|
| | $q_m$ (mmol $g^{-1}$) | $K_L$ | $q_m$ (mmol $g^{-1}$) | $K_L$ |
| Experimental | 17.87 | 0.088 | 2.14 | 133.35 |
| Model | 23.73 | 0.031 | 1.89 | 90.87 |

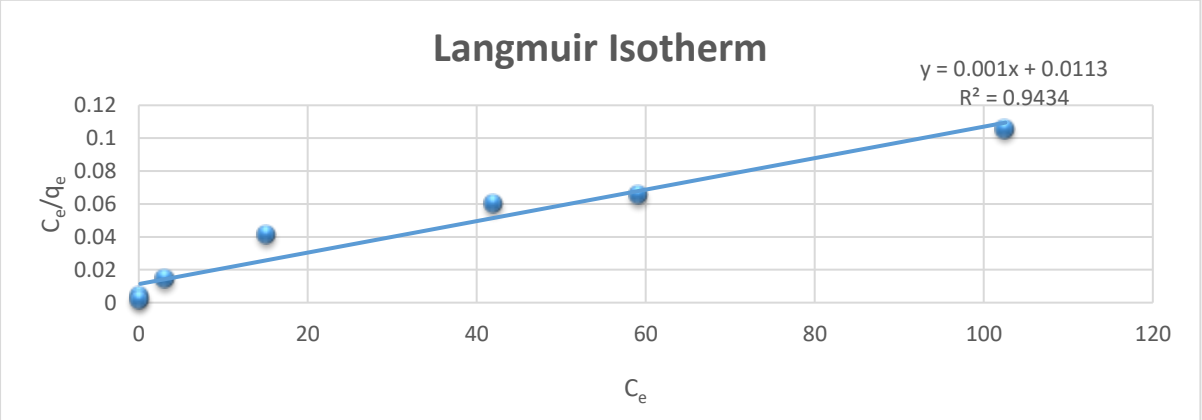


**Figure 32. Langmuir isotherm fitting for Mn.**

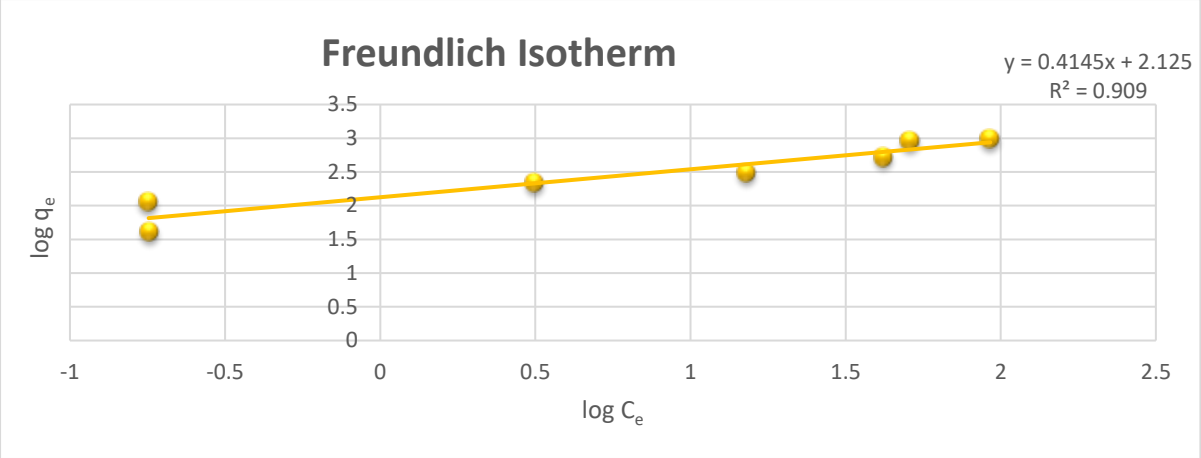


**Figure 33. Freundlich isotherm fitting for Mn.**

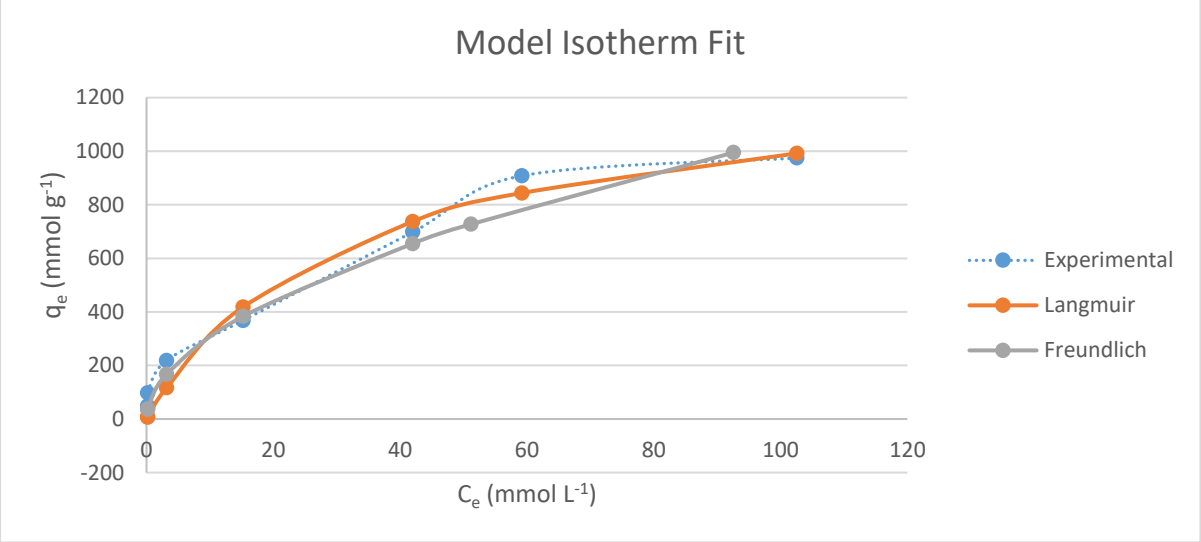


**Figure 34. Plots of qe(mg $g^{-1}$) versus Ce (mg $L^{-1}$) for Mn adsorption.**

Comparing all the results for adsorption capacity of RH2M towards metal ions (Fe, Cu, Zn, Mn and As), adsorption occurred by monolayer deposition except for As. As(III) showed relatively lower adsorption compared to other metal ions and also followed Freundlich isotherm model depicting multilayer deposition. This can be described by the slower adsorption time of As onto RH2M. As(III) required longer contact time while other metals were adsorbed quite rapidly. Due to increased contact time, the solution pH also increased and formation of more positive ions on the surface of adsorbent might have reduced the adsorption sites for As(III). Therefore, the adsorbed layer of As(III) ions acted as a novel active sites for remaining As(III) adsorption.

## 5.4. Column experiment

Synthesized iron nanoparticles containing adsorbent was further investigated for the removal of trace amount of uranium and other pollutants from natural and synthetic water by column experiment. Uranium is considered as the 38$^{th}$ prevalence element in the world with most of them captured inside sedimentary rocks as shale and carbonaceous phosphates. About 15 uranium minerals are used in industries, such as trivalent oxide of uranium, uranium silicates, phosphates and also complex compounds with titanium and vanadium (Maier et al., 2015).

Column experiment was performed with synthetic solution (S1) (Table 10) containing uranium with concentration of 20 $gL^{-1}$ that was fed into the column at the flow rate of 6 ml $min^{-1}$. The adsorbent mass used was 2 $gL^{-1}$, which was considered optimum from kinetic studies performed above.

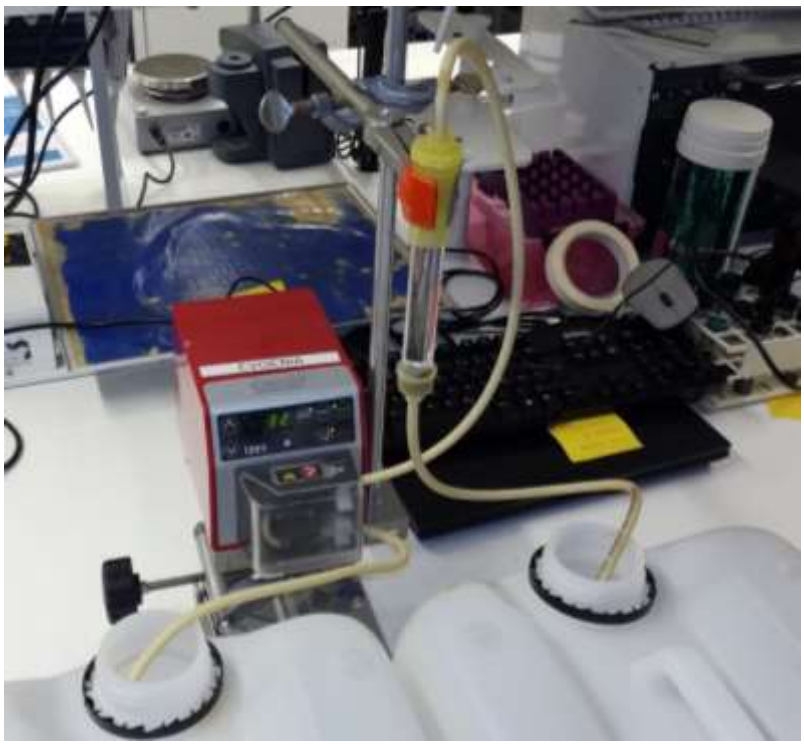

**Figure 35. Column experiment set up.**

The results are shown in table 12, which tells us that the removal of all the elements was quite significant with exception to copper and cadmium. Similar results on the influence of competing ions for available adsorption sites during uranium removal from multi-elemental

solution was also observed by (Borai et al., 2015) (Chen et al., 2016) (C. Jing, 2016). Adsorption of all other elements from synthetic solution was around 100%. However, removal percentage of cadmium and copper from solution was only about 60% and 80% respectively. This can be explained by possible competitive reactions between metal ions present in the solution for the available free sites of sorbent surface.

The possible mechanism of uranium removal shown in equations 5 and 6:

$$Fe - OH + UO_2^{2+} \rightarrow [(Fe - O)_2 UO_2] + H^+ \quad (5)$$

$$O - Si - O + UO_2^{2+} + H^+ + OH^- \rightarrow [(Si - O)_2 UO_2] + 2OH^- \quad (6)$$

In the both reactions equations, uranyl ions formed strong complexes with functional groups of sorbent. The chemical bonding of these complexes is so strong that the desorption of uranium/uranyl ions into solution was practically not observed.

**Table 12. Experimental results for synthetic solution (S1).**

| Elements | $C_i$ in S1, $mgL^{-1}$ | % Removal |
|---|---|---|
| Fe | 3000 | 100 |
| U | 20 | 99 |
| Pb | 10 | 99 |
| Cr | 200 | 99 |
| Zn | 250 | 99 |
| Cu | 100 | 80 |
| Cd | 5 | 60 |
| Mo | 10 | 99 |
| Se | 100 | 99 |

Synthetic solution S2 was prepared with very low concentration of uranium, close to that is present in natural water. Based on the results obtained from the column adsorption of S1, similar parameters were used for column adsorption test for synthetic solution S2 with uranium concentration of 0.02 $gL^{-1}$, and natural lake water. Results in table 13 show the amount of these trace elements adsorbed onto the RH2M adsorbent.

**Table 13.Experimental results for synthetic water (S2) and natural lake water.**

| Elements | C in solid sorbent after S2 treatment, mg $100L^{-1}$ | C in solid sorbent after natural water treatment, mg $100L^{-1}$ |
|---|---|---|
| Fe | 10000 | 10000 |
| U | 2.1 | 4.8 |
| Th | | 1.3 |
| Pb | 11.5 | 3.8 |
| Cr | 212 | 93 |
| Zn | 244 | 37 |
| Cu | 78 | 56 |
| Cd | 8.5 | 1.2 |
| Mo | 11.2 | 6.2 |
| Se | 106 | 118.3 |

Spectral analysis with TOF MS GD for sorbent after treatment of S2 and natural water are shown in figure 39 and 40 respectively. This spectral method more sensitive over other similar techniques allowing one to determine elements even in trace amount. This method provides an opportunity to analyze the samples for various isotopes of same element as shown in fig. 10 & 11. Fig. 11 also shows the isotope of $^{254}U$, adsorbed from natural water and concentrated on the sorbent surface. Uranium ($^{238}U$) is an technogenic isotope, which is found in spent nuclear fuel (Maier et al., 2015).

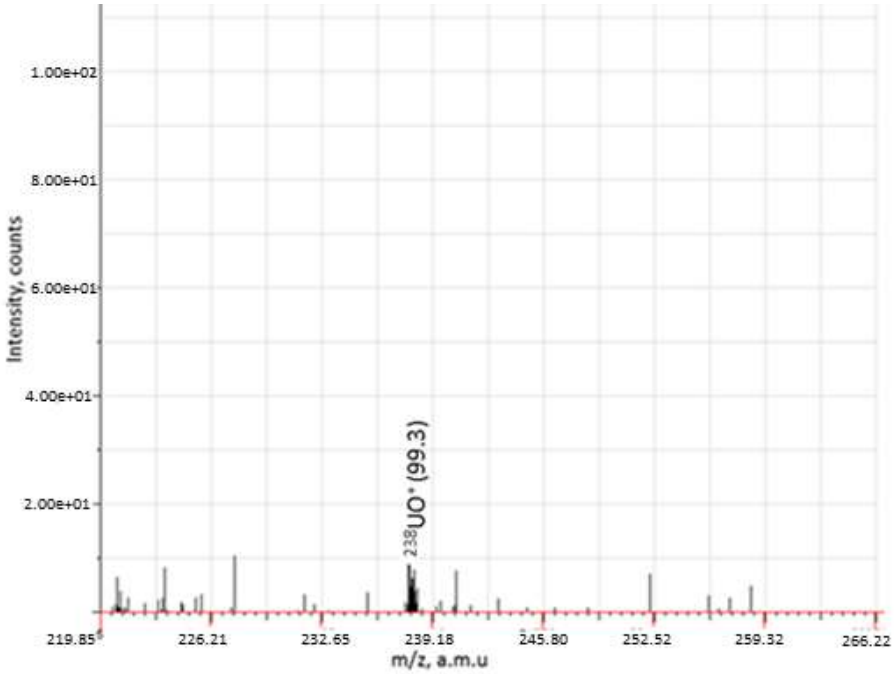


**Figure 36. Mass-spectral components of Uranium in sorbent after synthetic S2 water treatment with RH2M adsorbent.**

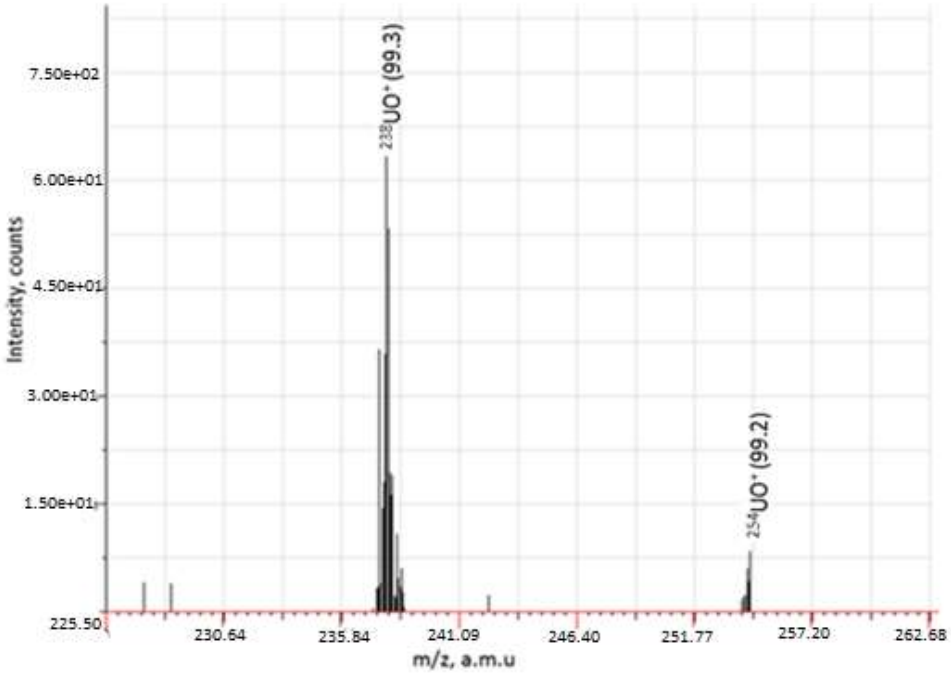


**Figure 37. Mass-spectral components of Uranium in sorbent after natural water treatment with RH2M adsorbent**

# 6. Conclusion

Wastewater treatment using low cost adsorbent is an area of interest to many researchers as it is presumed to provide double benefits: wastewater treatment and waste management. This research work followed similar trend to synthesize effective and low cost adsorbent from industrial waste. In this work, an industrial waste (industrial sand or RH) from Ekokem Finland Oy was used to synthesize iron nanoparticles containing low cost adsorbent for the removal of various metal ions from synthetic solution by adsorption.

Experimental results showed that it is very feasible to use this low cost adsorbent for the removal of metal ions from contaminated water. The adsorption capacity towards As, Fe, Cu, Mn and Zn was 1.07, 12.79, 15.73, 17.87 and 10.92 mmol $g^{-1}$ respectively. This values are competitive to the adsorption capacity of several commercial adsorbents. Optimum adsorption parameter from batch experiment was used to examine the removal efficiency of uranium ions from synthetic and natural water. Due to very low concentration of uranium in natural water, solid adsorbent after the adsorption test was analyzed using TOF MS. Results showed that about 4.8 mg $L^{-1}$ of uranium ($^{238}U$) was adsorbed from 100 L of natural lake water, which is quite promising result.

This study has shown the effectiveness of low cost adsorbent (RH) when applied for the adsorption of metal ions from contaminated water solution. The optimum adsorption parameters were estimated with synthetic solution. The adsorption capacity is quite good which can be compared to commercial adsorbents. This material has a great potential to be used as an adsorbent for acid mine drainage treatment. Moreover, less energy usage and low adsorbent cost is definitely an advantage of using this adsorbent.

## REFERENCES


1. Akcil A & Koldas S (2006). Acid Mine Drainage (AMD): causes, treatment and case studies. *Journal of Cleaner Production*, 14(12-13), 1139-1145.
2. Akdeniz Y & and Ulku S (2007). Microwave effect on ion-exchange and structure of clinoptilolite. *Journal of Porous Materials*, 14, 55-60.
3. Akin I, Arslan G, Tor A, Ersoz M & Cengeloglu Y (2012). Arsenic (IV) removal from underground water by magnetic nanoparticles synthesized from waste red mud. *Journal of Hazardous Materials*, 235-236, 62-68.
4. Akter KF, Owens G, Davey DE & Naidu R (2005). Arsenic Speciation and Toxicity in Biological Systems. *Rev Environ Contam Toxicol*, 184, 97-149.
5. Amini R, Rouhollahi A, Adibi M & Mehdinia A (2011). A novel reusable ionic liquid chemically bonded fused-silica fiber for headspace solid-phase microextraction/gas chromatography-flame ionization detection of methyl tert-butyl ether in a gasoline sample. *Journal of Chromatography A*, 1218, 130-136.
6. Bailey S, Olin T, Bricka R & Adrian D (1999). A review of potentially low-cost sorbents for heavy metals. *Water Research*, 33, 2469-2479.
7. Bhatnagar A & Minocha AK (2006). Coventional and non-coonventional adsorbents for removal of pollutants from water- *A review. Ind. J. of Chem. Tech*, 13, 203-217.
8. Bhatnagara A & Sillanpää M (2010). Utilization of agro-industrial and municiapl waste materials as potential adsorbents for water treatment-a review. *Chem Eng J*, 157, 49-55.
9. Bisht R, Agrawal M, & Singh K (2016). Heavy metal removal from wastewater using various adsorbents: a review. *Journal of Water Reuse and Desalination*, 7(1).
10. Borai E, Breky M, Sayed M & Abo-Aly M (2015). Synthesis, characterization and application of titanium oxide nanocomposites for removal of radioactive cesium, cobalt and europium ions. *Journal of Colloid and Interface Science*, 450, 17-25.
11. Brahmaiah T, Spurthi L, Chandrika K, Ramanaiah S & Prasad KS (2015). Kinetics of heavy metal (Cr & Ni) removal form the wastewater by using low cost adsorbent. *World Journal of Pharmacy and Pharmaceutical Sciences*, 4(11), 1600-1610.
12. Brunaeur S, Emmett P & Teller E (1938). Adsorption of gases in multimolecular layers. 309. *Bureau of Chemistry and soils and George Washington University*.
13. Buekens A & Zyaykina NN (2009). Adsorbents and adsorption processes for pollution control. *Pollution Control Technologies, II*.
14. C. Jing YL (2016). Review of soluble uranium removal by nanoscale zero valent iron. *Journal of Environmental radioactivity*, 164, 65-72.
15. Cabrera C, Gabaldon C & Marzal P (2005). Sorption characteristics of heavy metal ions by a natural zeolite. *Journal of Chemical Technology and Biotechnology*, 80, 477-481.
16. Castro H, Williams N & Ogram A (2000). Phylogeny of sulfate-reducing bacteria1. *FEMS Microbiology Ecology*, 31, 1-9.
17. CH2M Hill. (2010). Review of Available Technologies for the Removal of Selenium from Water. Retrieved from http://namc.org/docs/00062756.PDF.
18. Chen A, Shang C, Shao J, Zhang J & Huang H (2016). The application of iron-based technologies in uranium remediation: A review. *Science of the Total Environment.*

19. Chester A & Deroune E (2010). Zeolite characterization and catalysis: a tutorial. *Focus Catal*, 8.
20. Diaz-Teran J, Nevskaia D, Lopez-Peinado A & Jerez A (2001). Porosity and absorption properties of an activated charcoal, *Colloids and Surfaces A: Physiochemical and Engineering Aspects* (167-175), 187-188.
*21.* Envirogen Technologies. (2011). Treatment of Selenium-Containing Coal Mining Wastewater with Fluidized Bed Reactor Technology. *An Envirogen Technologies Whitepaper.*
22. EPA. (2014). Reference guide to treatment technologies for mining-influenced water. *United States Environmental Protection Agency*.
23. EPA. (2016). Abandoned Mine Drainage. Retrieved 03 13, 2017, from https://www.epa.gov/nps/abandoned-mine-drainage
24. Evangelou V (1998). Pyrite chemistry: the key for abatement of acid mine drainage. *In Acidic Mining Lakes: Acid Mine Drainage, Limnology and Reclamation* (pp. 197-222). Berlin: Springer.
25. Filippis PD, Palma LD, Petrucci E, Scarsella M & Verdone N (2013). Production and Characterization of Adsorbent Materials from Sewage Sludge by Pyrolysis. *The Italian Association of Chemical Engineering*, 32. doi:10.3303/CET1332035
26. Gaikwad R, Misel W, Dhirendra S & Gupta D (2011). Removal of metal from acid mine drainage (AMD) by using natural zeolite of Nizarneshwar Hills of Western India. *Aarbian Journal of Geosiciences*, 4(1), 85-89.
27. Ghali EO (2014). Treatment of fe-containing acidic mine waters in fixed bed adsorption column with calcite side- stones. Lappeenranta: *Lappeenranta University of Technology.*
28. Giles C, Nakhwa SN, Smith D & MacEwan TH (1960). Studies in Adsorption. Part XI. A system of classification of solution Adsorption Isotherms and its use in Diagnosis of Adsorption Mechanisms and in Measurement of Specific Surface Area of Solids. *Journal of Chemical Society*, 3973-3993.
29. Gregg S & Sing K (1982). *Adsorption, Surface Area and Porosity* (2nd ed.). London: Academic Press.
30. Hamza A & Fashola SO (2014). Calcined iron rich clay as an adsorbent and a photocatalyst for the degradation of phenol. *Nigerian Journal of Technological Research,* 9(2).
31. Hasley G (1952). The role of surface heterogeneity. *Adv. Catal*, 4, 259-269.
32. Haunch S (2013). The legacy of historic mining and water quality in a heavily mined Scottish river catchment. Edinburgh: College of Science and Engineering at the *University of Edinburgh*.
33. Holmes J & Kreusch E (1972). Acid Mine Drainage Treatment by Ion Exchange. Washington: *U.S. Environmental Protection Agency*.
34. Iakovleva E & Sillanpää M (2013). The use of low-cost adsorbents for waste water purification in mining industries. *Eviron Sci Pollut Res*. doi:10.1007/s11356-013-1546-8

35. Iakovleva E, Mäkilä E, Salonen J, Sitarz M, Wang S & Sillanpää M (2015). Acid mine drainage (AMD) treatment: Neutralization and toxic elements removal with unmodified and modified limestone. *Ecological Engineering*, 81, 30-40.
36. Iakovleva E, Maydannik P, Ivanova TV, Sillanpää M, Tang WZ, Mäkilä E, Wang, S (2016). Modified and unmodified low cost iron containing solid wastes as adsorbents for efficient removal of As(III) and As(IV) from mine water. *Journal of Cleaner Production*, 133, 1095-1104.
37. Inglezakis V, Diamandis N, Loizidou M & Grigoropoulou H (1999). Effect of pore clogging on kinetics of lead uptake by clinoptilolite. *Journal of Colloid and Interface Science*, 215, 54-57.
38. ITRC. (2005). Permeable Reactive Barriers: Lessons Learned/New Directions. Washington, D.C.: *Interstate Technology Regulatory Council*.
39. ITRC. (2008). Mine Waste Issues in the United States: A White Paper. Retrieved 3 18, 2017, from http://www.itrcweb.org/team_Resources_mining/MiningWhitePaper_2008.pdf.
40. ITRC. (2010). Mining Waste Treatment Technology Selection Website. Retrieved 3 18, 2017, from http://www.itrcweb.org/miningwaste-guidance/
41. Jolivet J, Chaneac C & Tronc E (2004). Iron oxide chemistry: From molecular clusters to extended solid networks. *Chemical communications*, 481-487.
42. Kagambega N, Sawadogo S, Bamba O, Zombre P & Galvez R (2014). Acid mine drainage and heavy metals contamination of surface water and soil in southwest burkina faso–west Africa*. International Journal of Multidisciplinary Academic Research*, 2(3), 9-19.
43. Kauppila P, Räisänen ML & Myllyoja S (2011). Best Environmental Practises in Metal Ore Mining. *Finnish Environmental Institute.*
*44.* Kepler D & McCleary E (1994). Successive alkalinity-producing systems (SAPS) for the treatment of acidic mine drainage. Pittsburgh, PA: *Proceedings of the International Land Reclamation and Mine Drainage Conference.*
45. Kikuchi S & Tanaka T (2012). Biological removal and recovery of toxic heavy metals in water environment. *Crit Rev Environ Sci Technol*, 42, 1007-1057.
46. Kimmel W (1983). The impact of acid mine drainage on the stream ecosystem. In Pennssylvania coal, resources, technology and utilization. In S. M. Miller (Ed.), *The Pa. Acad. Sci. Publ.* (pp. 424-427).
47. Kirby D (2014). Effective treatment options for acid mine drainage in the coal region of west virginia. Marshall: *Marshall University.*
48. Kleiman GG & Landman U (1973). Theory of Physisorption: He on Metals. *Physical Review B*, 8(12).
49. Laurent S, Forge D, Port M, Roch A, Robic C, Elst LV & Muller RN (2008). Magnetic Iron Oxide Nanoparticles: Synthesis, Stabilization, Vectorization, Physicochemical Characterizations and Biological Applications. *Chem. Rev,* 108, 2064-2110.
50. Machado S, Grosso J, Nouws H, Albergaria J & Delerue-Matos C (2014). Utilization of food industry wastes for the production of zero-valent iron nanoparticles. *Science of the Total Environment*, 496, 233-240.
51. Macingova E & Luptakova A (2012). Recovery of Metals from Acid Mine Drainage. *Chemical Engineering Transactions*, 28, 109-114.

52. Maier W, Lahtinen R & O'Brien H (2015). Mineral Deposits of Finland. *Elsevier*.
53. Massaro E J (2002). Handbook of Copper Pharmacology and Toxicology. New Jersey: *Humana Press Inc.*
54. Matlock MM, Howerton BS & Atwood DA (2002). Chemical precipitation of heavy metals form acid mine drainage. *Water Research*, 36(19), 4757-4764.
55. Merta E (2015 11 3). Adsorption. Retrieved 9 28, 2016, from http://wiki.gtk.fi/web/mine-closedure/wiki/-/wiki/Wiki/Adsorption/pop_up;jsessionid=4295298309237fc27c51b671415f
56. Misawa T, Hashimoto K & Shimodaira S (1974). The mechanism of formation of iron oxide and oxyhydroxides in aqueous solutions at room temperature. *Corrosion Science,* 14, 131-149.
57. Monte FD, Morales MP, Levy D, Fernandez A, Ocana M, Roig A, Serna C (1997). *Langmuir*, 13, 3627.
58. Motsi T (2010). Remediation of acid mine drainage using natural zeolite. Birmingham, UK: School of Chemical Engineering, *The University of Birmingham*.
59. Motsi T, Rowson NA & Simmons MJ (2009). Adsorption of heavy metals from acid mine drainage by natural zeolite*. International Journal of Mineral Processing*, 92, 42-48.
60. Mukherjee R, Sinha A, Lama Y & Kumar V (2015). Utilization of zero valent iron particles produced from steel industry waste for in-situ remediation of ground water contaminated with organo-chlorine pesticide heptachlor. *Int. J. Env. Res*, 9(1), 19-26.
61. Mullett M, Fornarelli R & Ralph D (2014). Nanofiltration of Mine Water: Impact of Feed pH and Membrane Charge on Resource Recovery and Water Discharge. *Membranes (Basel)*, 4(2), 163-180.
62. Naffrechoux E & Hamdaouia O (2007). Modeling of adsorption isotherms of phenol and chlorophenols onto granular activated carbon part I. Two-parameter models and equations allowing determination of thermodynamics parameters. *Journal of hazard. material*, 147, 381-394.
63. Natarajan E & Ponnaiah GP (2010). Synthesis of Iron Oxide Micro and Nanoparticles from Aluminum Industry Waste and Its Application in the Decolorization of Reactive Blue 235 Dye. *Current Pharmaceutical Biotechnology*, 17(10), 873-885.
64. NCKU (2015). Chapter 9 Adsorption. Retrieved 21.09.2016, from http://www.che.ncku.edu.tw/facultyweb/leeyl/94%20%E7%95%8C%E9%9D%A2%E7%8F%BE%E8%B1%A1/Chapter%2009%20Adsorption.pdf
65. Nguyen TV, Nguyen TV, Pham, TL & Nguyen DT (2009). Adsorption and removal of arsenic from water by iron ore mining waste. *Water Science & Technology*, 60(9), 2301-2308.
66. Nguyen YS, Gupta BS & Hashim MA (2016). Performance evaluation of natural iron-rich sandy soil as a low-cost adsorbent for removal of lead from water. *Desalination and Water Treatment*, 57(11), 5013-5024.
*67.* Oleksiienko O (2016). Physio-chemcial properties of sol-gel synthesized titanosilicates for the uptake of radionuclides from aqueous solutions. Mikkeli: *Lappeenranta University of Technology.*
68. Panek R, Franus W & Wdowin M (2011). Hydrothermal inversion of F class fly ash into synthetic zeolites. *Abstract Book IS. AM&MM*.

69. Patagonia (2007). Double threat of Cyanide Leach Mining and Acid Mine Drainage (AMD) imperils the Futaleufu River Valley - Kinross Gold & Geocom Resources responsible. Retrieved 9 30, 2016, from http://patagonia-under-siege.blogspot.fi/2007/12/double-threat-of-cyanide-leach-mining.html
70. Phuengprasop T, Sittiwong J & Unob F (2011). Removal of heavy metal ions by iron oxide coated sewage sludge. *Journal of Hazard Material*, 186, 502-507.
71. Pozo-Antonio S, Puente-Luna I, Laguela-Lopez S & Veiga-Rios M (2014). Techniques to correct and prevent acid mine drainage. *Dyna rev.fac.nac.minas*, 81(186).
72. Rani B, Singh U & Maheshwari R (2011). Ecologically Engineered Strategies for the Management of Acid Mine Drainage: An Overview. *Journal of Advanced Scientific Research*, 2(3), 6-9.
73. Reichl C, Schatz M & Zsak G (2016). WORLD-MINING-DATA. Vienna: Federal Ministry of Science, *Research and Economy*, Austria.
74. Reinsel M (15.1.2016). Water online. Retrieved 28.09.2016, from http://www.wateronline.com/doc/selenium-removal-technologies-a-review-0001
75. Repo E, Malinen L, Koivula R, Harjula R & Sillanpää M (2011). Capture of Co(II) from its EDTA-chelate by DPTA-modified silica gel and chitosan. *Journal of Hazardous Materials*, 187, 122-132.
76. Repo E, Warchol J, Bhatnagar A & Sillanpää M (2011). Heavy metals adsorption by novel EDTA-modified chitosan-silica hybrid materials. *Journal of Colloid Interface*, 358, 261-267.
77. Rios C, Williams C & Roberts C (2008). Removal of heavy metals from acid mine drainage (AMD) using coal fly ash, natural clinker and synthetic zeolites. *Journal of Hazardous Materials*, 156(1-3), 23-35.
78. Sangita GU & Prasad B (2010). Studies on Environmental Impact of Acid Mine Drainage Generation and its Treatment; An Appraisal. IJEP, 30(11), 953-967.
79. Saria L, Shimaoka T & Miyawaki K (2006). Leaching of heavy metals in acid mine drainage. *Waste Man. Res*. 24(2), 134-140.
80. Satyawali Y & Balakrishnan M (2008). Wastewater treatment in molasses-based alcohol distilleries for COD and color removal: A review. *Journal of Environmental Management*, 86, 481-497.
81. Sheoran A & Sheoran V (2006). Heavy metal removal mechanism of acid mine drainage in wetlands: A critical review. *Minerals Engineering*, 19(2), 105-116.
82. Silva A, Lima M, Rosa MF & Versiane LA (2012). Mine water treatment with limestone for sulfate removal. *Journal of Hazardous Materials*, 221-222, 45-55.
83. Singer P & Strumm W (1970). Acid mine drainage. Science (New York), 167, 1121-1123.
84. Skousen, J. (1991). Anoxic limestone drains for acid mine drainage treatment. *Green Lands,* 21(4), 30-35.
85. Skousen JG, Sextone A & Ziemkiewicz PF (2000). Acid Mine Drainage Control and Treatment. -In: Barnishal, R. I, Darmody, R. G. & Daniels, W. L. In Reclamation of Drastically Distributed Lands (6) (pp. 131-168). Madison: Wis. (*American Society of Agronomy*).
86. Soto M, Moure A, Domínguez H & Parajó J (2011). Recovery, concentration and purification of phenolic compounds by adsorption: a review. *J Food Eng*, 105(1), 1-27.

87. Stoeckli H, Guillot A, Slasli A & Hugi-Cleary D (2002). The comparison of experimental and calculated pore size distributions of activated carbons. *Carbon*, 40, 383-388.
88. Strosnider W & Nairn R (2010). Effective passive treatment of high-strength acid mine drainage and raw municipal wastewater in Potosí, Bolivia using simple mutual incubations and limestone. *J. Geochem. Explor*, 105, 34-42.
89. Sun S & Zeng H (2002). Size-Controlled synthesis of Magnetic Nanoparticles. *J. Am. Chem. Soc*, 124(28), 8204-8205.
90. Sweeney D (2005). U.S environmental protection agency. (sosbluewaters) Retrieved 19.09.2016, from http://www.sosbluewaters.org/epa-what-is-acid-mine-drainage[1].pdf
*91.* Taylor J, Pape S & Murphy N (2005). A Summary of Passive and Active Treatment Technologies for Acid and Metalliferous Drainage (AMD). Fremantle, Western Australia: *Earth Systems PTY LTD.*
92. Tekes (2012). The Global Industrial Waste Recycling Markets. Helsinki: *Tekes*.
93. Tripathi A & Ranjan MR (2015). Heavy metal removal from wastewater using low cost adsorbents. *Journal of Bioremediation and Biodegradation*, 6(315).
94. Turner D & McCoy D (1990). Anoxic alkaline drain treatment system, a low cost acid mine drainage treatment alternative. In Proc. of the National Symp. on Mining (pp. 73-75). Lexington, KY: *Uni. of Kentucky*.
95. USEPA (2000). Interstate Technology Regulatory Council. USEPA.
96. Van der Wal A, Norde W, Zehnder A & Lyklema J (1997). Determination of the total charge in the cell walls of Gram-positive bacteria. *Colloids and Surfaces B: Biointerfaces*, 9, 81-100.
97. Varanada L, Morales M, Jafelicci M & Serna C (2002). Monodispersed spindle-type geothite nanoparticles from FeIII solutions. *Journal of materials chemistry*, 12, 3649-3653.
98. Vijayaraghavan K & Yun YS (2008). Bacterial biosorbents and biosorption. *Biotechnology Advances*, 26, 266-291.
99. Watten B, Sibrell P & Schwartz M (2005). Acid neutralization within limestone sand reactors receiving coal mine drainage. *Environ. Poll*, 137, 295-304.
100. Weider RK & Lang GE (1982). Modification of Acid Mine Drainage in a Freshwater Wetland. Proceedings of the Symposium on Wetlands of the Unglaciated Appalachian Region. Morgantown: *West Virginia University*.
101. Wolkersdorfer C (2008). Mine Water Treatment and Groundwater Protection. In Water Management at Abandoned Flooded Underground Mines (pp. 235-275). Munchen, Germany: *LE-TEX Jelonek, Schmidt & Vockler GbR*, Leipzig, Germany.
102. Worch E (2012). Isotherm equations for single-solute adsorption. In E. Worch, Adsorption Technology in Water Treatment (pp. 46-47). Berlin: *Walter de Gruyter GmbH & Co.*
103. Yavuz CT, Mayo JT, Yu WW, Prakash A, Faulkner JC, YeanS, Colvin VL (2006). Low-field Magnetic Separation of Monodisperse Fe3O4 Nanocrystals. *Science*, 314, 964-967.
104. Zielinski JM & Kettle L (2013). Physical Characterization: Surface Area and Porosity. Allentown, Manchester: Intertek.

105. Zipper C, Skousen J & Jage C (2011). Passive treatment of acid mine drainage. Virginia: Virginia Polytechnic Institute and State University.